Faux Vector Processor Design Using FPGA-Based Cores

by
Diwas Timilsina

A thesis submitted in partial fulfillment
of the requirements for the
Degree of Bachelor of Arts with Honors
in Computer Science

Williams College
Williamstown, Massachusetts

May 22, 2016

Contents

List of Figures

List of Tables

Listings

Acknowledgement

I would like to express my sincere gratitude to my advisor Prof. Duane Bailey for the continuous support of my undergraduate study and research, for his patience, motivation, enthusiasm, and immense knowledge. His guidance helped me in all the time of research and writing of this thesis.

Besides my advisor, I would like to thank my second reader: Prof. Tom Murtagh, and the entire Williams College Computer Science department for their encouragement, insightful comments, and hard questions.

Abstract

Roughly a decade ago, computing performance hit a *power wall*. With this came the power consumption and heat dissipation concerns that have forced the semiconductor industry to radically change its course, shifting focus from performance to power efficiency. We believe that Field programmable gate arrays (FPGAs) play an important role in this new era. FPGAs combine the performance and power savings of specialized hardware while maintaining the flexibility of general purpose processors (GPPs). Most importantly, pairing an FPGAs with a GPP to support *partnered computation* can yield performance and energy efficiency improvements, and flexibility that neither device can achieve on their own. In this work, we show that a GPP tightly coupled to a sequential vector processor implemented on an FPGA, called *Faux Vector Processor* (FVP), can support efficient, general purpose, partnered computation.

1. Introduction

Microprocessor performance has increased dramatically over the past few decades. Until recently, Gordon E. Moore's famous observation that the number of transistors on *integrated circuits* (IC[1]) doubles roughly every 12-18 months (Moore's law) has continued unabated. The driving force behind Moore's law is the continuous improvement of the *complementary metal oxide semiconductor* (CMOS) transistor technology, the basic building block of digital electronic circuits. CMOS scaling has not only led to more transistors but also to faster devices (shorter delay times and accordingly higher frequencies) that consume less energy. During this period of growth, every generation of processor supported chips with twice as many transistors, executing of about 40% faster and consuming roughly the same total power as the previous generation [23]. The theory behind this technology scaling was formulated by Dennard et al. [7] and is known as *Dennard scaling*. There was a time when Dennard scaling accurately reflected what was happening in the semiconductor industry. Unfortunately, those times have passed.

As the performance of processors improved due to shrinking transistors, the supply voltage of the transistors was not dropping at the same rate. As a direct consequence, chip power consumption grew with increased performance gains until only a decade ago. Higher power consumption results from current leakage, producing more heat. Power consumption and heat dissipation concerns have now forced the semiconductor industry to stop pushing clock frequencies further, effectively placing a tight limit on the total chip power. As a result, the frequency scaling driven by shrinking transistors has hit the so-called *power wall*. This trend is captured in Figure 1.1. In this new era, with each successive processor generation, the percentage of a chip that can switch at full frequency is dropping exponentially due to power constraints. Experiments conducted by Venkatesh et al. from UCSD show that we can switch fewer than 7% of transistors on a chip at full frequency while remaining under a power budget [27]. This percentage will decrease with each processor generation [27]. This underutilization of transistors due to power consumption constraints is called *dark silicon*.

[1] A table of acronyms can be found beginning on page 68.

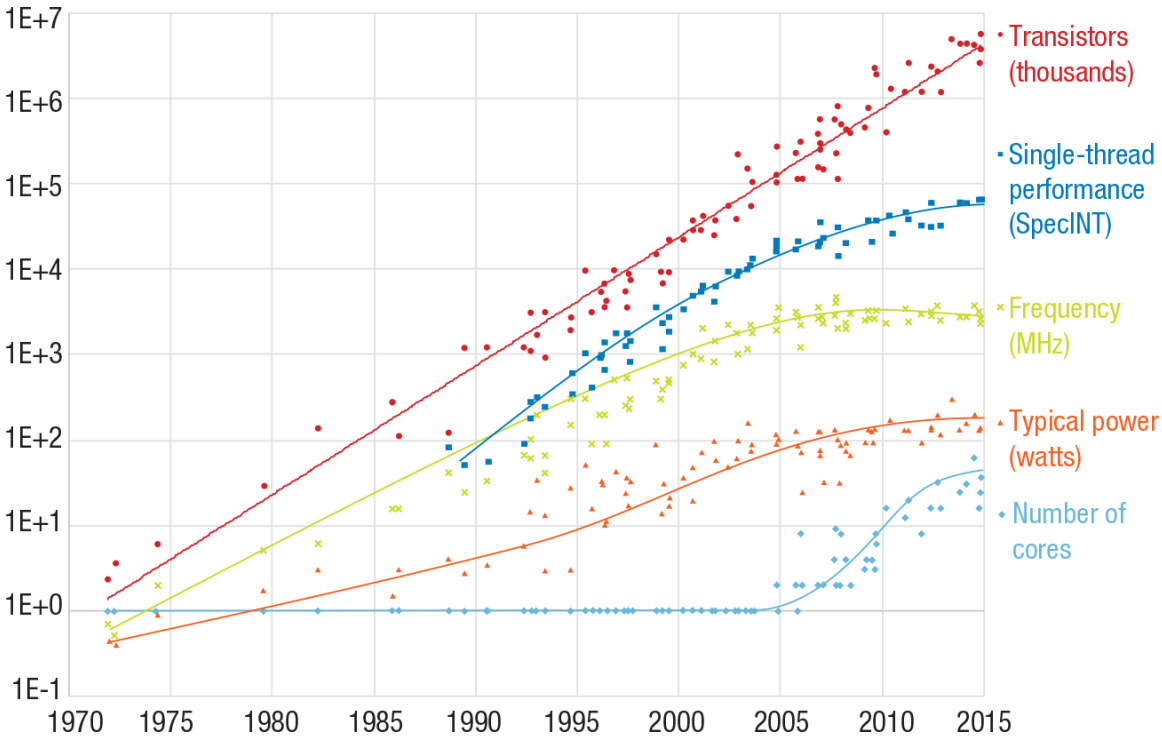

Figure 1.1: 40 Years of trend in microprocessor data. Figure from Moore [23].

There are several approaches to building more power efficient architectures to tackle dark silicon. Traditionally engineers have achieved performance and energy improvements by using special purpose *application specific integrated circuits* (ASICs). ASICs are designed for a particular use. The biggest downside of dedicated ASICs is their inflexibility. Another promising way to overcome these limitations is to move towards heterogeneous architectures, where cores vary and tasks are off-loaded to specialized hardware. The specialized core will better at performing specialized computation and consume a lot less power. Effectively, enabling the hybrid architecture to stay under the power budget and utilize the silicon that would have dark. One way to build such hybrid architecture is to use a *general purpose processor* (GPP) with a set of tightly coupled ASIC co-processors. ASICs are designed for a particular use and are more efficient that GPPs as they do not need to include components for instruction decode. Graphic processors are an example of this approach. UCSD's *Conservation Core* project also demonstrated significant energy efficiency with this approach [27], but the approach inherits the inflexibility of ASIC-based design. The static nature of the ASIC cores makes it an impractical target when the codebase for the specific application changes. An alternative approach of building these heterogeneous architectures is to replace the ASIC like cores with reconfigurable cores. Reconfigurable cores provide

a compromise between GPPs and ASICs. *Field Programmable Gate Arrays* (FPGAs) are ideal candidates for the reconfigurable cores. While FPGAs are generally less computationally powerful than GPPs, they are more flexible than ASICs. Therefore, FPGA-based heterogeneous circuits consume moderate power, allow multiple specialized circuits to be "loaded" whenever they are needed, drastically reduce time-to-market, and also provide the ability to upgrade already deployed circuits. Of course, there is no free lunch: building heterogeneous architectures with FPGAs is a difficult and time-consuming process.

In this work, we explore the trade offs in designing a partnered computation pairing a GPP with a FPGA based vector processor. Unlike a typical vector processor, our vector processor will be optimized towards power efficiency rather than performance. Leading hardware manufactures are also starting to realize the possibility of FPGA based co-processors [11]. Intel, leading chip manufacture, recently announced that it is working to produce a GPP with a tightly coupled FPGA based processors. While FPGAs have made significant advances and are now highly capable, the software and documentation supporting them is still primitive. Therefore, in this work we also use the vector processor as a target architecture to take step closer towards mitigating the difficulties in programming FPGA to make it more accessible to programmers.

The rest of the chapters are organized as follows. Chapter 2 goes over the previous work on energy efficiency; comparison between GPPs, ASICs, and FPGAs; FPGA-based vector processors; heterogeneous co-processor systems; and power analysis on FPGA. Chapter 3 describes the traditional FPGA project workflow by walking through an example. In Chapter 4, we present the design and goals of our FPGA-based *faux vector processor* (FVP), followed by Chapter 5 that outlines our methodology for evaluating our design and describes our results. Chapter 6 suggests some options for future exploration. Finally, Chapter 7 briefly summarizes our findings.

2. Previous Work

Previous research related to this work can be grouped into four main categories. First, there is a large body of research focused on relative efficiency of computation performed on GPPs, FPGAs, and ASICs. Second, there has been significant work on improving the performance of conventional vector processors and also on designs that include vector processors as co-processors. Third, there have been a number of attempts to design performance enhancing hardware designs. Finally, there is a small body of research focused on power analysis and optimization on FPGAs. We consider these contributions in this section.

2.1 Efficiency Comparison Between GPPs, FPGAs, and ASICs

In this section, we'll look at previous works focused on the efficiency comparison between GPPs, FPGAs, and ASICs that informed our research on the benefits of using FPGA based cores.

Hill and Marty of University of Wisconsin extend Amdahl's simple software model and compute performance speedup for symmetric, asymmetric, and dynamic multicore chips [13]. Amdahl's software model is used to find the maximum expected improvement to an overall system when only part of the system is improved. Symmetric processors dedicate the same resources to each multicore (e.g. 16 identical 4-resource multicores on a 64-resource chip), asymmetric processors have differently sized cores (e.g. one 16-resource core and 24 2-resource cores), and dynamic processors can be run-time reconfigured to run as one powerful core for sequential processing or as a set of possibly asymmetric smaller cores for parallel processing. Even though multicore processors do not have application specific hardware, asymmetric multicores represent a similar approach to that of ASICs: trying to break up the larger computation into pieces that can be handled by optimally-sized sections of hardware. Their key conclusion is that in terms of performance, the dynamic multicore designs outperform asymmetric multicores, and asymmetric multicore designs perform better than symmetric ones. Similar to Hill and Marty's work, Woo and Lee of Georgia Institute

of Technology extend Amdahl's law and develop analytcial power models for symmetric, asymmetric, and dynamic chip design to evaluate energy efficiency on the basis of power models [29]. Their analysis demonstrates that symmetric and asymmetric multicore chips can easily lose their energy efficiency as the number of cores increases. Their work concludes that a dynamic multicore processor with many small energy efficient cores integrated with a single larger core provides the best energy efficiency.

Hameed et al. analyze the inefficiencies of GPPs compared to ASICs [12]. According to their findings, GPPs spend over 90% of their computation on instruction fetch and decode and only 10% on computation as shown in Figure 2.1. Their results show that such overhead can be completely eliminated by using ASICs. ASICs are generally around 50× more efficient than GPPs both in terms of power and performance because they can exploit parallelism, group complex instructions that are often used together, and make use of specialized hardware specifically designed for a target application. In this way, the authors claim that a truly efficient design will require application-specialized hardware.

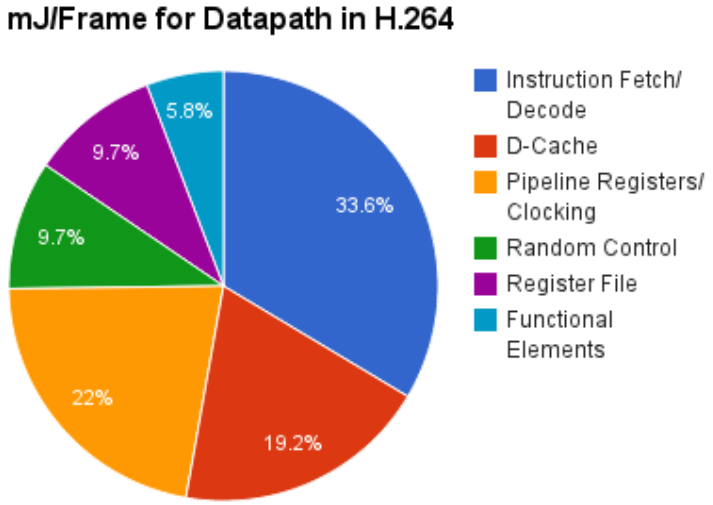

Figure 2.1: Chart of GPP computation energy. Roughly 5% of computation energy goes to the functional units, with most being spent on computational overhead. Data from Hameed et al. [12]

Kuon and Rose's work on measuring the performance and energy gap between FPGAs and ASICs describes the empirical measurements of the difference between a 90-nm CMOS FPGA and 90-nm standard-cell ASIC in terms of logic density, circuit speed and power consumption. Their results show that FPGA logic requires roughly 35× more area (mostly due to routing), 14× more power, and a 3-4× longer critical path. Most modern FPGAs have some hard logic blocks (arithmetic logic units (ALUs), random access memory (RAM)

blocks, etc.), which can reduce those gaps to around 18× for area, and 8× for power with only minor impact on the delay, depending on how much of the application hardware can be mapped to those hard blocks. The cost of those improvements is the loss of flexibility on the FPGA, as fabric space must be dedicated to the hard blocks, whether or not they are used.

Chung et al. raise an interesting question in their work: "Does the future of chip design include custom logic, FPGAs, and General Purpose Graphic Processor Units (GPGPUs)?"[4]. They weigh the benefits and trade-offs associated with integrating unconventional cores (u-cores) with GPPs to reach their conclusion that future chip design should include custom logic. Since power consumption and I/O bandwidth are the two main performance bottlenecks for modern computation, the authors evaluate three different types of u-cores, namely ASICs, FPGAs, and GPGPUs, paired with GPPs in terms of energy efficiency rather than pure performance. To accurately measure the energy efficiency, sequential operations are performed on the GPP and parallel operations are performed on the u-cores. Their results show that u-cores almost always improve the efficiency of computation, especially as the amount of parallelism in the target application increases. Further, the benefits of u-core use are heavily dependent on off-chip bandwidth trends. This is because bandwidth ceilings quickly become a limiting factor for extremely fast custom logic. Even if I/O and bandwidth improvements continue to lag behind logic improvements, FPGAs will be able to offer performance that is closer to that of ASICs than their relative computational efficiency would suggest. The authors conclude that ASICs offer both the highest performance and the most power efficiency, but that ASICs are expensive to develop and designed around a single set of target applications. On the other hand, FPGAs can provide significant efficiency gains over GPPs alone while offering more flexibility than ASICs.

2.2 The Return of the Vector Processor

A vector processor is a processor that can operate on an entire vector in one instruction. The operand to the instructions are complete vectors instead of single elements. Vector processors reduce the fetch and decode bandwidth as fewer instructions are fetched. They may also exploit data parallelism in applications. The difference between scalar and vector architecture is described in Figure 2.2. In this section, we describe the previous contributions that motivated our research to choose vector processors as the co-processor in our design.

In their 2002 paper, Kozyrakis and Patterson describe the Vector Intelligent RAM (VIRAM)

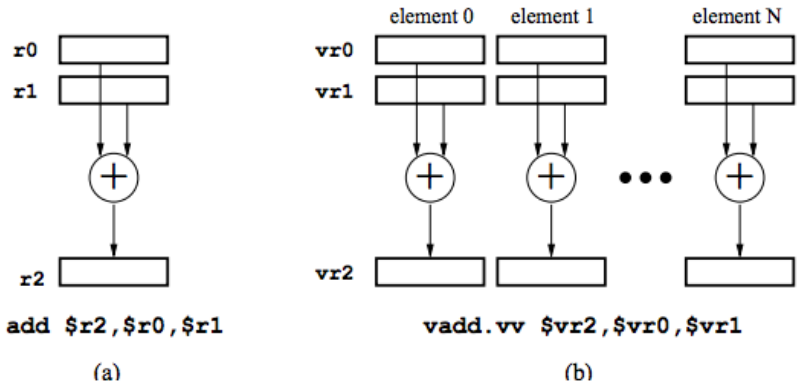

Figure 2.2: The difference between scalar and vector instructions. A scalar instruction (a) defines a single operation on a pair of scalar operands. An addition instruction reads two individual numbers and produces a single sum. On the other hand, a vector instruction (b) defines a set of identical operations on the elements of two linear arrays of numbers. A vector addition instruction reads two vector operands, performs element-wise addition, and produces a similar array of sums. Figure from Kozyrakis and Patterson [17]

architecture aimed at developing a vector processor that provides high performance for multimedia tasks at low energy consumption [17]. The VIRAM micro-architecture relies on two basic technologies: vector processing and embedded DRAM. The vector architecture allows for high performance for multimedia applications by executing multiple element operations in parallel, and the embedded DRAM enables the integration of a large amount of DRAM memory on the same die with the processor. The vector hardware executes the VIRAM instruction set (a standard, straightforward extension of MIPS instruction set), connects to the scalar MIPS core as coprocessor, and operates at a modest speed of 200 MHz. The MIPS core supplies the vector instructions to the vector lanes for in-order execution, and vector load and store instructions access DRAM-based memory directly without using SRAM caches. The design partitions the register and data path resources in the vector coprocessor vertically into four lanes. Figure 2.3 shows the block diagram for the VIRAM architecture with its four components: the MIPS scalar core, the vector co-processor, the embedded DRAM main memory, and the external IO interface. Overall, the authors are able to show that VIRAM architecture is more energy efficient and less complex than VLIW architecture and super scalar architecture. However, they claim that VIRAM is susceptible to the basic limitations of traditional vector designs: (1) the complexity and size of the centralized vector register file that limits the number of functional units, (2) the difficulty of implementing precise exceptions for vector instructions, and (3) the high cost

of vector memory systems.

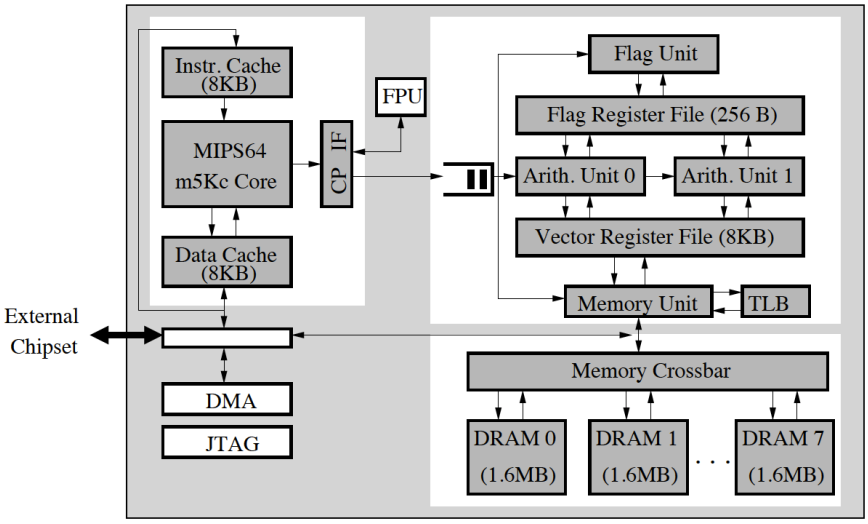

Figure 2.3: Figure showing the block diagram of VIRAM architecture. Figure from Kozyrakis and Patterson [17]

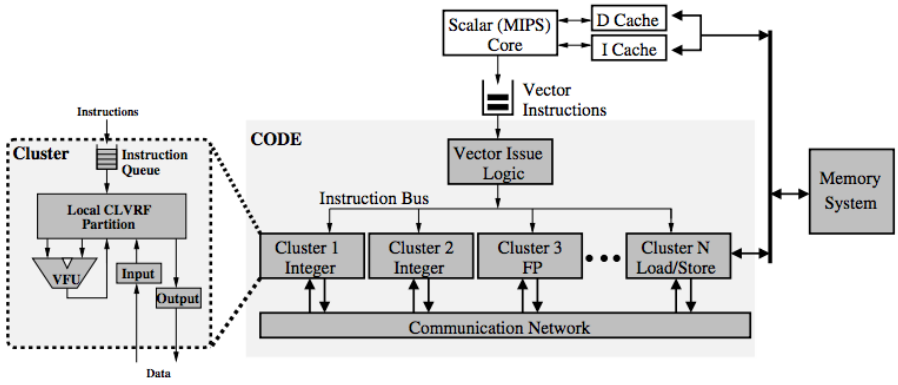

Figure 2.4: Figure showing the block diagram of CODE architecture. Figure from Kozyrakis and Patterson [18]

In their 2003 followup paper, Kozyrakis and Patterson attempt to address the limitations of VIRAM architecture by introducing an improved micro-architecture called Cluster organization for Decoupled Execution (CODE) [18]. CODE differs from the VIRAM micro-architecture in two ways. First, it breaks up the centralized register file and distributes the vector registers across all cores. Second, it uses decoupling, instead of the delayed pipeline, to tolerate long memory latencies. VIRAM structures the vector coprocessor around a cen-

tralized vector register file that provides operands to all functional units and connects them to each other. In contrast, the composite approach organizes vector hardware as a collection of interconnected cores. Each core is a simple vector processor with a set of local vector registers and one functional unit. Each core can execute only a subset of the instruction set. For example, one vector core may be able to execute all integer arithmetic instructions, while another core handles vector load and store operations. The composite organization breaks up the centralized vector register file into a distributed structure, and uses renaming logic to map the vector registers defined in the VIRAM architecture to the distributed register file. The composite organization uses a communication network for communication and data exchange between vector cores, as there is no centralized register file to provide the functionality of an all-to-all crossbar for vector operands. The block diagram of CODE is shown in Figure 2.4. Their results show that CODE is 26% faster than a VIRAM with a centralized vector register file that occupies approximately the same die area. They are also able to show that CODE only suffers less than 5% performance loss due to precise exception support. Most importantly, CODE is able to scale the vector coprocessor in a flexible manner by mixing the proper number and type of vector cores. If the typical workload for a specific implementation includes a large number of integer operations, more vector cores for integer instruction execution could be allocated. Similarly, if floating-point operations are not necessary, all cores for floating-point instructions could be removed. In contrast, with VIRAM one could only increase performance by allocating extra lanes, which evenly scales integer and floating-point capabilities, regardless of the specific needs of applications. Yu et al. demonstrate the potential for vector processing as a simple-to-use and salable accelerator for soft processors [34]. Their architecture consists of a scalar core (single threaded version of 32-bit Nios II), a vector processing unit, and a memory unit. The scalar core and the vector unit share the same instruction memory and the same instruction fetch logic. The scalar and vector units can execute instructions in parallel and also can coordinate via a FIFO queue for instructions requiring both cores. The vector unit is a VIRAM based vector architecture extended to take advantage of on chip memory blocks and hardware multiply accumulate (MAC) units common in FPGAs. The vector unit is composed of a specified number of vector lanes, each with complete copies of a functional unit, partition of the vector register file and vector flag registers, load store unit, and local memory. Through performance modeling the authors are able to show that a vector processor can potentially accelerate data parallel benchmarks with performance scaling better than Altera's behavioral synthesis tool even after manual code restructuring. Further, they are also able to show how FPGA architectural features can be exploited to provide efficient support for some vector operations. For example, the multiply-accumulate blocks internally sum multiple partial products from narrow multiplier circuits to implement wider multiplication

operations. Figure 2.5 shows the block diagram of vector component of their soft core architecture.

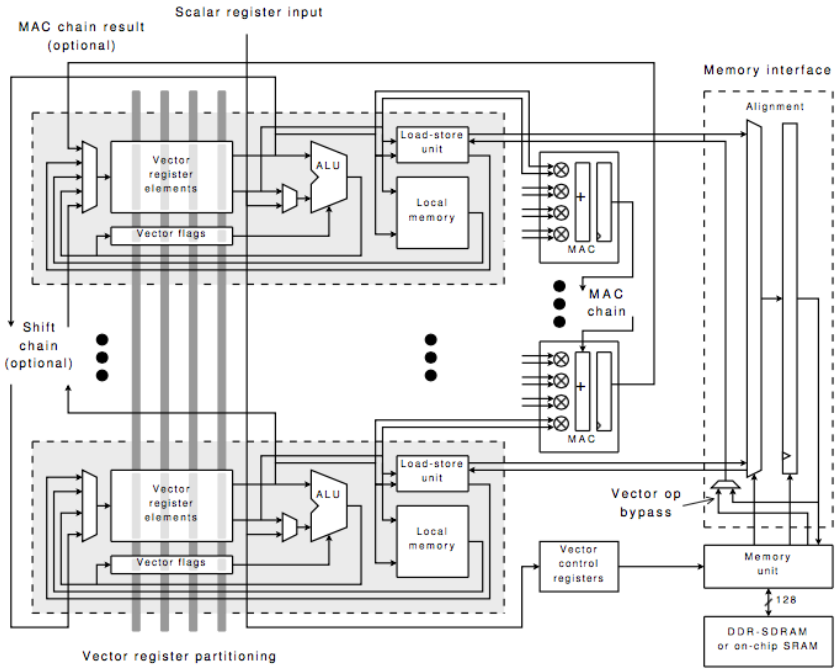

Figure 2.5: Figure showing the block diagram of vector coprocessor in soft core processor architecture. Figure from Yu et al. [34]

Yiannacouras et al. extend this work by proposing a full and verified hardware implementation of a soft vector processor called Vector Extended Soft Processor Architecture (VESPA), connected to off-chip memory, and with GNU assembler vector support [32]. VESPA is a MIPS-based scalar processor with a highly configurable VIRAM-like vector coprocessor implemented using Stratix III FPGA. The scalar and the vector coprocessors share the same instruction cache, and both cores can execute out-of-order with respect to each other except for communication and memory instructions which are serialized to maintain sequential memory consistency. VESPA architecture is composed of three pipelines. Figure 2.6 shows the VESPA pipelines with each stage separated by black vertical bars. The topmost pipeline is the three-stage scalar MIPS processor discussed earlier. The middle pipeline is a simple three-stage pipeline for accessing vector control registers and communicating between the scalar processor and vector coprocessor. The actual vector instructions are executed in the longer seven-stage pipeline at the bottom of Figure 2.6. Vector instructions are first decoded and proceed to the replicate pipeline stage which divides the elements of work requested by

the vector instruction into smaller groups that are mapped onto the available lanes. VESPA is also a highly configurable design as all parameters are built-in to the Verilog design so a user need only enter the parameter value and have the correct configuration synthesized with no additional source modifications. With VESPA, Yiannacouras et al. are not only able to show that their architecture can scale performance from 1.8× up to 6.3×, but also automatically generate application-specific vector processors with reduced datapath width and instructions set support which combined reduce the area by 70% without affecting performance.

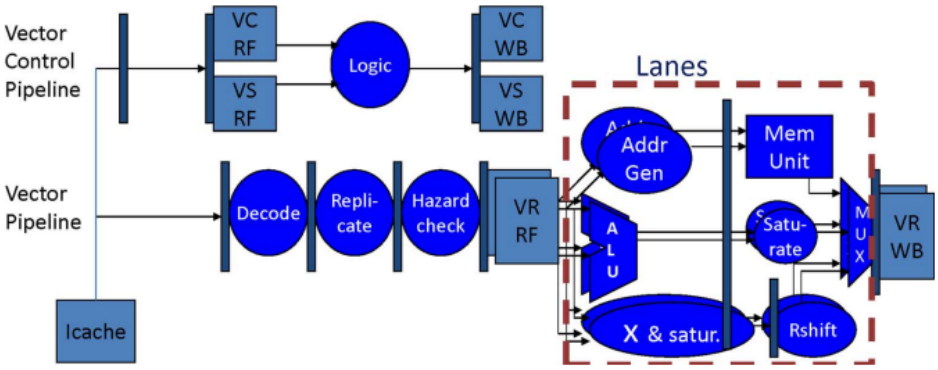

Figure 2.6: VESPA architecture with two lanes. The black vertical bars indicate pipeline stages, the darker blocks indicate logic, and the light boxes indicate storage elements for the caches as well as the vector control (vc), vector scalar (vs), and vector (vr) register files. Figure from Yiannacouras et al. [32]

Ciricescu et al. describe a vector coprocessor accelerator architecture called the Reconfigurable Streaming Vector Processor (RSVP) that improves the performance of streaming data. RSVP uses a stream oriented approach to vector processing by decoupling and overlapping data access and data processing. There are several load/store units that prefetch vector data from long-latency, wide memory and turn it into narrow, high speed streams of vector elements, that communicate with the processing units via an interlocked FIFO queue. RSVP uses a programming model that separates data from computation; data is described by location and shape in the memory and computation is described using machine independent data flow graphs. Figure 2.7 shows the block diagram of vector component of their soft core architecture. The white components are visible to the programmer while the grey components represent data-flow computation structure that is hidden from the programmer. Overall, the authors are able to show that RSVP achieves speedups for kernels and applications range from 2 to over 20× that of a host processor alone, and is easy to

market because of the ease of programmability.

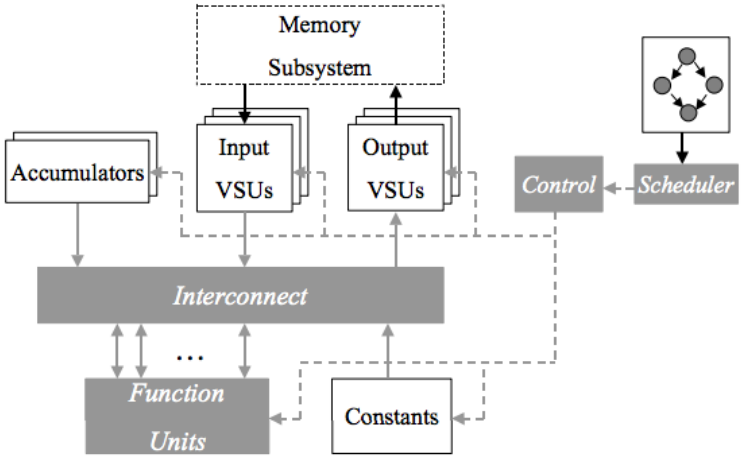

Figure 2.7: The RSVP Architecture. Figure from Ciricescu et al. [5]

2.3 Performance- and Power-Improving Designs

In this section, we look at specialized hardware designed for performance and energy efficiency. The architectures discussed in this section are hybrid systems with a GPP tightly coupled with one or more co-processing units. The architectural choices described in these contributions have motivated important design decisions in our design.

In 2010, Venkatesh et al. from UCSD analyzed the benefits of pairing specialized conservation cores (c-cores) with GPPs with the aim of significantly reducing the power consumption for frequently executed, energy intensive code [27]. As described in Chapter 1, the frequency-scaling power wall has made energy efficiency, rather than pure computational speed, the primary bottleneck. They argue that if a given computation can be made to consume less power at the same level of performance, then other computations can be run in parallel without violating the power budget. As a result, their primary focus is not increased performance, but rather similar performance with lower energy consumption. Because they target energy efficiency, rather than computation speed, c-cores can be used for a much broader set of applications or code blocks, even when there is no available parallelism to exploit. Even when there is not parallelism to be exploited (or when acceleration via increased parallelism is not the goal), using c-cores simply to make computation more energy efficient is worthwhile because it allows more of the chip to be functional at any given time. The c-core system, as described, contains multiple tiles, each of which contains one GPP and several heterogeneous c-cores as shown in Figure 2.8. The researchers' toolchain

generates c-cores by profiling a target workload, selecting "hot" code regions, and automatically synthesizing c-core hardware to implement the code block. The compiler must be extended to use available c-cores on applicable code segments, while executing other code on the GPP. The researchers also discuss "patchable" c-cores, which are more flexible (increasing their lifetime and the amount of code they can execute) but incur 2× area and power consumption overhead. Their results suggest that a system using 18 c-cores can have a 16× improvement in energy consumption for code that can be executed on the c-cores, resulting in a reduction of nearly 50% for the energy consumption of the target applications as a whole.

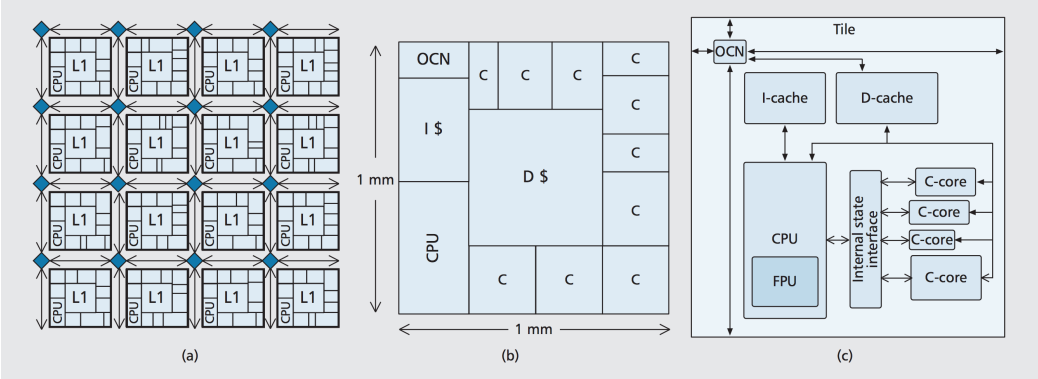

Figure 2.8: A diagram showing (a) a c-core chip with multiple tiles, (b) the physical floorplan for an individual tile, and (c) the logical layout of the interconnects within a tile. Figure from Goulding-Hotta et al. [10]

Canis et al. present an open source, high-level synthesis tool called LegUp that leverages software techniques for hardware design[3, 2]. Their design allows users to explore the hardware/software design space. Using the architecture some portion of a program can run on a GPP, and others can be implemented as custom hardware circuits. LegUp takes a standard C program as an input and automatically compiles the program to a hybrid architecture containing a FPGA-based MIPS soft processor and custom hardware accelerators that communicate through a standard bus interface. Their design flow comprises first compiling and running a program on a standard processor, profiling its execution, and then recompiling the program to a hybrid hardware/software system. In their design, they leverage the LLVM compiler framework for high-level language parsing and its standard compiler optimization [20]. Figure 2.9 shows the detailed design flow for LegUp. Their architecture can synthesize most of the C language to hardware, like fixed-sized multi-dimensional arrays, structs, global variables and pointer arithmetic. However, dynamic memory, floating point, and recursion is not supported by their architecture. Overall, compared to software running on

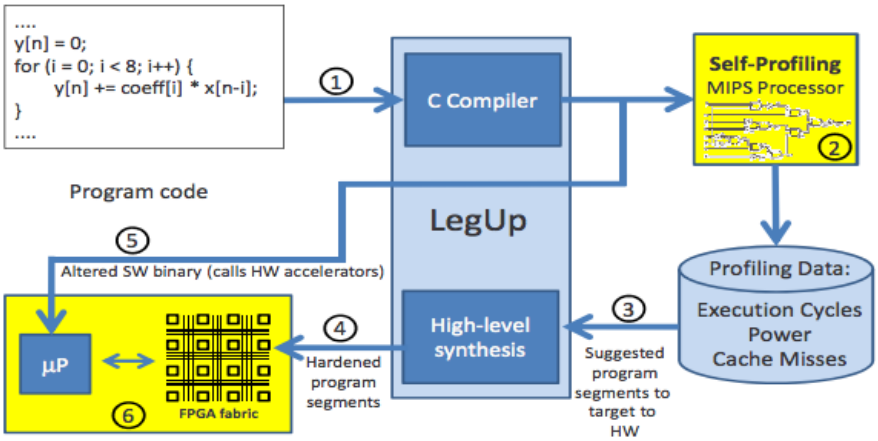

Figure 2.9: The Block diagram showing LegUp design. Figure from Canis et al. [2]

a MIPS soft processor, hybrid architecture provided by LegUp execute 8× faster and use 18× less energy.

2.4 GPP-FPGA Communication

While FPGA technology seems so promising, we can not fully realize the potential of FPGA-GPP architecture without having some form of interface between the logic fabric and the computer program running on the GPP. In this section, we look at some of the contributions made in this field.

Jacobsen and Kastner from UCSD designed a reusable integration framework for FPGA accelerators called Reusable Integration Framework for FPGA Accelerators (RIFFA) [14]. RIFFA is a simple framework for communicating data from a host CPU to a FPGA via a PCI express bus. RIFFA is an alternative to Xillybus, which is used in our project. The framework requires a PCIe enabled workstation and a FPGA on a board with a PCIe connector. RIFFA supports Windows and Linux, Altera and Xilinx, with bindings for C/C++, Python, MATLAB and Java. On the software side there are two main functions: data send and data receive. These functions are exposed via user libraries in C/C++, Python, MATLAB, and Java. The driver supports multiple FPGAs (up to 5) per system. The software bindings work on Linux and Windows operating systems. On the hardware side, users access an interface with independent transmit and receive signals. The signals provide transaction handshaking and a first word fall through FIFO interface for reading/writing data. No knowledge of bus addresses, buffer sizes, or PCIe packet formats is required. RIFFA

does not rely on a PCIe bridge and therefore is not subject to the limitations of a bridge implementation. Instead, RIFFA works directly with the PCIe endpoint and can run fast enough to saturate the PCIe link. Their experiments show that RIFFA can achieve 80% of the theoretical bandwidth of data transfer between host CPU and FPGA over PCI bus in nearly all cases. Figure 2.10 shows the block diagram of the RIFFA architecture. The downside in their architecture is that the details of PCIe protocol device driver, DMA operation, and all hardware addressing are hidden from the software and hardware in their architecture. As a result some user flexibility is lost because of the design choice.

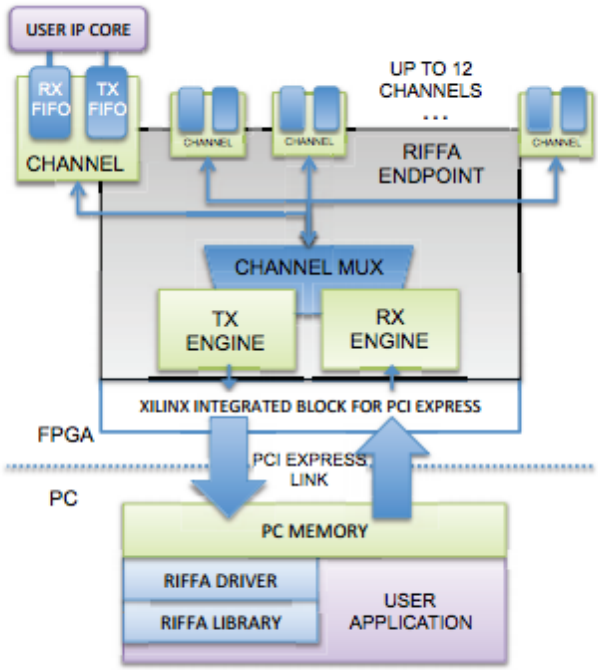

Figure 2.10: RIFFA 2.0 architecture. Figure from Jacobsen and Kastner [14]

Similar to RIFFA, Connectal by King et al. from Quanta Research Cambridge is a software driven hardware development framework which aims to narrow the boundary between the software and hardware development using FPGA [16]. Their hardware components are written in Bluespec System Verilog (BSV) and the software components are implemented in C/C++. Using BSV, their architecture allows users to declare logical groups of unidirectional "send" methods, each of which is implemented as a FIFO channel; all channels corresponding to a single BSV interface are grouped together into a single "portal". The hardware and software communicate with each other using these portals. Overall, their framework connects software and hardware by compiling interface declaration, allows con-

current access to hardware accelerators from software, allows high-bandwidth sharing of system memory with the hardware accelerators, and also provides portability across different platforms.

In 2015, Fleming et al. from Imperial College of London, present a system-level linker called PushPush, which allows functions in hardware and software to be linked together to create heterogeneous systems[8, 25]. PushPush links together pre-compiled modules from different compute domains and languages, called "system objects". System objects are modules which export a set of functions and also may import functions from others. They can be software functions, classes, libraries, or intellectual property (IP) cores in hardware. Design flow of their architecture is shown in Figure 2.11.

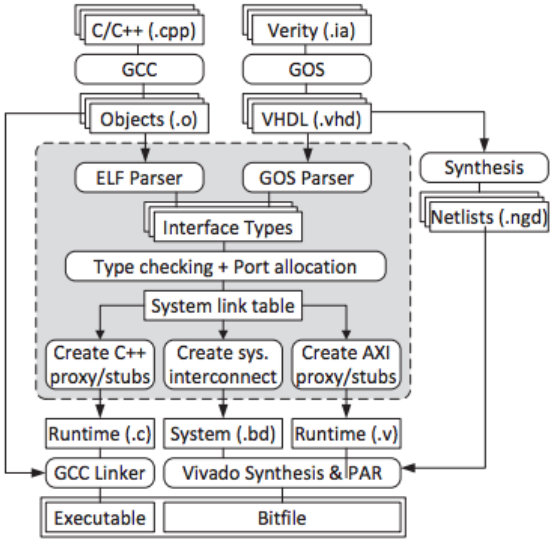

Figure 2.11: Design flow diagram for PushPush linker. Figure from Fleming et al. [8]

The system linker is shown in gray and it takes in software and hardware object files to be linked as input. At the next step, the type information is parsed out of the binary files using ELF information in the software binary or Verity's equivalent meta-data. All function names and types are then merged and similar checks as that of software linker (eg type checking) are performed. All symbols are resolved to one exporter and zero or more importers. At the next stage, proxies and stubs are added on both hardware and software sides, and linking code is generated that connects imported symbols in one module to exported symbols in another. In the final stage, all the components are combined. The software side is linked together with the standard linker bringing together the user's software and the system linker's proxies and stubs. For hardware, the system linker generates an

IP block incorporating the CPU, user's hardware, and the Advanced eXtensible Interface (AXI) proxies and stubs. The final result is a single executable containing both software and hardware. The researchers also built a fully functional and automated prototype on the Zynq platform and are able to show that this type of linking enables a more equal partnership between hardware and software, with hardware not just acting like a "dumb accelerator" but also being able to initiate execution across the system.

2.5 Power Consumption Analysis on FPGA

Analysis and estimation for power dissipation of FPGAs has received little attention compared to that of standard cell ASIC. Most of this limited research on FPGA power consumption have focused primarily on dynamic power consumption. There has been very little work to estimate and analyze static power consumption of FPGAs. In this section, we discuss some of the work done towards analyzing both dynamic and static power consumption on an FPGA. These contributions will serve as a reference for power analysis of our design in later chapters.

Tuan and Lai from Xilinx Research Lab and UCLA analyze the leakage power of a low-cost 90nm FPGA using detailed device-level simulation. There simulations are performed using DC operating point analysis in SPICE. DC operating point analysis calculates the behavior of a circuit when a DC voltage or current is applied to it. The result of this analysis is generally referred as the bias point, quiescent point or Q-point. The author's measurement methodology is based on measuring the power consumption by configurable logic blocks (CLBs), building block of the FPGA circuit. The authors first divide the CLBs into smaller circuit blocks. Next, each block is simulated individually to identify its leakage power consumption. As the FPGA architecture is highly regular, iterating over all the circuit blocks is quite manageable. The total leakage power of the CLB array is then computed by taking the sum of each block's leakage power. Finally, this total power consumed by CLB array is multiplied by the number of CLBs in the array to get the total leakage power. To model the effect of input variation, the simulation is performed under all possible input states of circuit blocks. Using this methodology, they found that their FPGA consumes 4.2μW static power per CLB under normal conditions and more than 26μW per CLB in the worst case. The authors conclude that there is a potential for substantial leakage reduction through optimization of basic circuits and power management based on resource utilization.

Shang et al. from Princeton University and Xilinx Research Lab analyze the dynamic power consumption in an FPGA by taking advantage of both simulation and measurement. The

target device for this project is a Xilinx Virtex-II. According to the authors, the total power dissipation is a function of three factors. First is the effective capacitance, which is defined as the "parasitic" effect due to interconnection wires and transistors, and the emulated capacitance because of short-circuit current. The effective capicatance of each resource is computed using direct measurement and SPICE simulation. The second factor is the resource utilization, i.e the proportion of look up tables (LUTs), block RAMs (BRAMs) etc used in circuit design. Finally, the most important factor determining the power dissipation is the switching activity. Switching activity is defined as the number of signal transitions in a clock period. Resource utilization and switching activity is computed using software called Modelsim. The authors model these factors as follows

$$P = \frac{1}{2} V^2 f \sum_i C_i U_i S_i$$

where V is the supply voltage, f is the operating frequency, and C_i, U_i, S_i are the effective capacitance, utilization, and switching activity of each resource, respectively. Using this equation, the authors compute the power dissipation of few benchmark circuits. According to their results most of the power dissipation occurs in the interconnection resources. The authors also conclude that for the xilinx Vertex-II FPGA operating at 100MHz with input voltage of 1.5V, each CLB would consume 5.9μW per MHz.

There has been considerable work on dynamic power analysis on FPGAs. Degalahal and Tuan model dynamic power consumption of FPGA based on clock power, switching activity, and dominant interconnect capacitance. Similarly, Jevtic and Carreras present a measurement model that separately measures clock, interconnect, and logic power to compute the total dynamic power consumed by the FPGA. These are some direct ways of measuring power consumption on an FPGA. An alternative to this approach is to rely on power analysis software to measure the power consumption. For the purpose of this project, we relied on Vivado's power analysis tool to measure the power consumption of our design, and are aware that better estimates are possible.

2.6 Summary

The computational performance of a chip has hit a power wall [27]. As a result, it is becoming increasingly difficult to improve energy efficiency while maintaining computational performance. A lot of work has been done to evaluate the performance and energy efficiency of ASICs, FPGAs, and GPPs to determine the right architecture for the job. The past works comparing different kinds of heterogeneous processors have shown that

even though ASICs have a considerable performance advantage compared to FPGAs, FPGAs can be significantly more efficient than general purpose processors while maintaining enough flexibility to be used for a wide variety of applications. Furthermore, designs that combine heterogeneous accelerators with GPPs make it clear that such a design can offer significant flexiblity with performance and efficiency gains compared to a GPP, ASIC, or FPGA alone. The c-core and QS-core research [27, 28] suggests that a system integrating automatically generated ASICs with a modified compiler and runtime controller can significantly reduce power consumption. Similarly, the RIFFA, PushPush, and Connectal research [3, 8, 16] have shown that a system integrating FPGA with a modified runtime controller can significantly improve power and performance efficiency. These efforts have focused on trading execution of instruction for hardware, and mostly neglect the possibility to harness the power of parallelism. Previous works on vector processors have shown the possibility to solve the problem through parallelism. The projects like VIRAM, VESPA, CODE, RSVP [17, 18, 32, 5] have made it clear that vectors processors can be very efficient co-processors and can provide significant performance and energy boost. Works described in this section suggests that a heterogeneous design with a GPP tightly coupled with one or many reconfigurable co-processors would yield significant energy efficiency gains while maintaining flexibility.

3. The FPGA Work Flow

Since FPGAs provide a compromise between the performance of ASICs and the flexibility of GPPs, the FPGA seems an ideal partner for a GPP. The Xilinx Zynq-7000 is one such heterogeneous computing platform used in this project. It integrates a dual-core Cortex A9 ARM processor and an FPGA inside one chip. Moreover, because of its tightly-coupled processing system (PS) and programmable logic (PL), the Xilinx's Zynq seems to be an ideal platform on which to implement a configurable co-processor. Figure 3.1 shows a picture the Xilinx's Zynq-7000 ZedBoard Evaluation Kit. Before we consider our proposed architecture, we describe the architecture of an FPGA, typical workflow for programming an FPGA, and the pros-and-cons of the tools encountered.

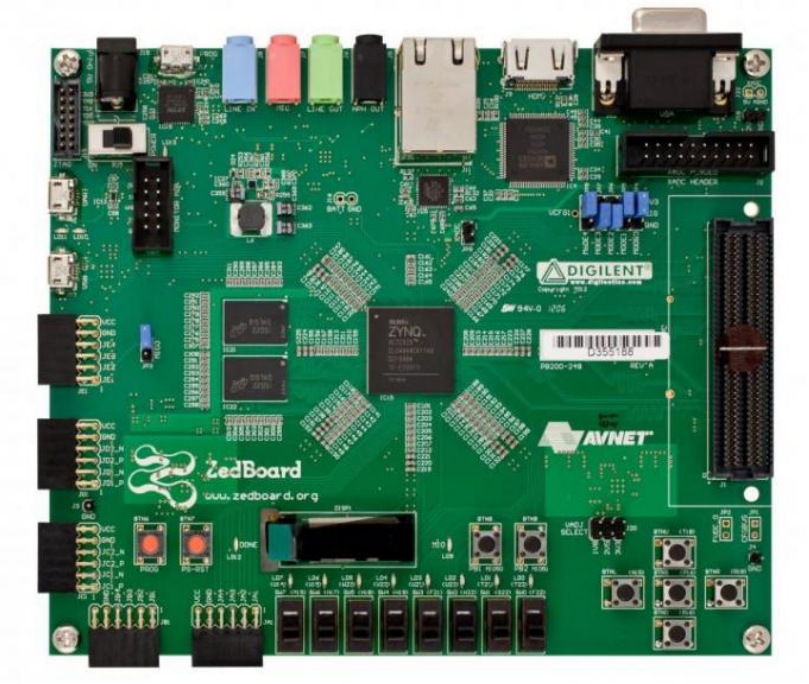

Figure 3.1: Xillnx's Zedboard. Figure from Zedboard's Website[35]

3.1 Field Programmable Gate Array Architecture

In this section, we give an overview of the technology behind field programmable gate arrays (FPGAs). FPGAs arose from programmable logic devices (PLDs), which first appeared in early 1970s. However, these early FPGAs were very limited as programmable logic was hardwired between logic gates. In 1985, the first commercially available FPGA (the Xilinx XC2064) hosted arrays of *configurable logic blocks* (CLBs) that contained *programmable gates* as well as *programmable interconnect* between the CLBs. Since then FPGAs have rapidly evolved.

Now, most FPGAs are composed of three fundamental components: combinational logic (compute), memory elements (storage), and a programmable interconnect (communication). In custom ASIC, combinational logic is built by wiring a number of physical basic logic gates together. In FPGAs, these logic gates are simulated using multiple instances of a generic configurable element called a *look-up-table* (LUT). An n-input LUT can be used to implement an arbitrary deterministic function with up to n inputs. Each LUT is paired with a flip-flop (FF). This facilitates pipelined circuit design, where signals may propagate through large part of the FPGA chip. LUTs can also be configured to support, in parts, as *distributed RAM* (Memory LUTs in Xilinx architecture).

A fixed number of LUTs are grouped and embedded into a programmable logic component called *elementary logic unit*. Xilinx refers these units as *slices* in their architecture. The exact architecture of elementary logic units varies among different vendors and even between different generations of FPGAs from the same vendor. Nevertheless, we can identify four main structural elements: LUTs (usually between two to eight), registers, arithmetic/carry logic, and multiplexers. A small number of these elementary logic units are grouped together into a coarser grained *logic island*, or configurable logic block (CLB).

The *interconnect* is a configurable routing architecture that allows communication between arbitrary logic islands. It consists of communication channels (bundles of wires) that run horizontally and vertically across the chip, forming a Manhattan-style grid. Where routing channels intersect, *programmable links* determine how signals are routed. As illustrated in Figure 3.2, the two-dimensional array of communication logic islands is surrounded by I/O blocks (IOBs). These IOBs, at the periphery of the FPGA, connect the programmable interconnect to the adjacent circuitry.

The logic resources of FPGAs discussed so far are, in principle, sufficient to implement a

wide range of circuits. However, to address high performance and usability needs, FPGA vendors additionally intersperse FPGAs with special silicon components such as *block RAMs* (BRAMs) and *digital signal processors* (DSP units). BRAMs can hold comparatively large amount of data making them ideal choice to store large amount of working data on-chip. DSP units contain dedicated hardware to support arithmetic signal processing, including high performance multipliers and adders. These are a few examples of embedded silicon components on FPGAs. Often FPGA vendors add more complex hardwired circuitry to their FPGAs to support common functionality at high performance with minimal chip space and power consumption. Having discussed the key components of FPGAs, we now consider how FPGAs are programmed.

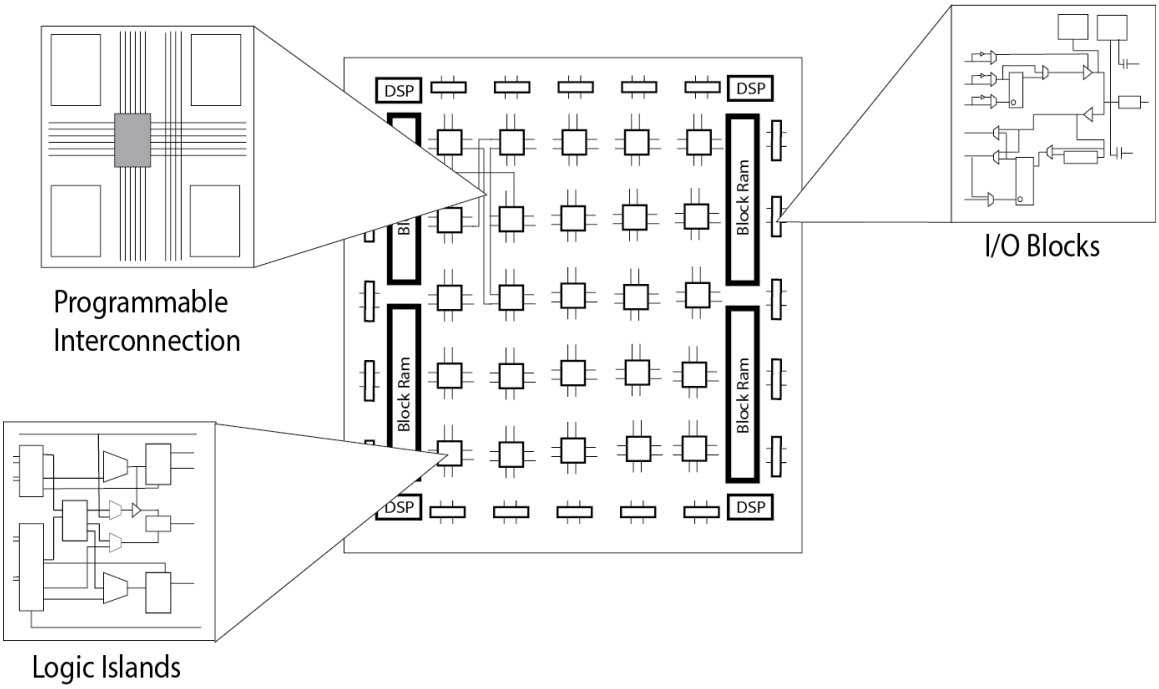

Figure 3.2: Block diagram showing FPGA layout.

3.2 Architecture Supporting Partnered Communication

One of the daunting tasks in FPGA design is effectively communicate with adjacent processors. Implementing the low-level bus protocols is a project in itself. In this work, we used a pre-packaged communication solution, Xillybus, to allow us to focus our efforts on co-processor design.

Xillybus consists of an IP core and a Linux driver. IP cores are the FPGA equivalent of library functions. IP cores may implement certain mathematical functions, a functional unit (example, a USB interface), an entire processor (e.g. ARM). They promote hardware design reuse. Managed by linux driver, Xillybus forms a kit for elementary data transport between an FPGA and the host, providing pipe-like data streams with a relatively straightforward user interface. It is intended as a low-effort solution for mixed partnered computations like ours, where it makes sense to have the project-specific part of the driver running as a user-space process. On the host side, the FPGA looks like a character device file. On the FPGA side, hardware FIFOs are used to control the data stream. Figure 3.3 shows how the FPGA interacts with the ARM processor. The Xillybus core on the Zynq operates at 100 MHz.

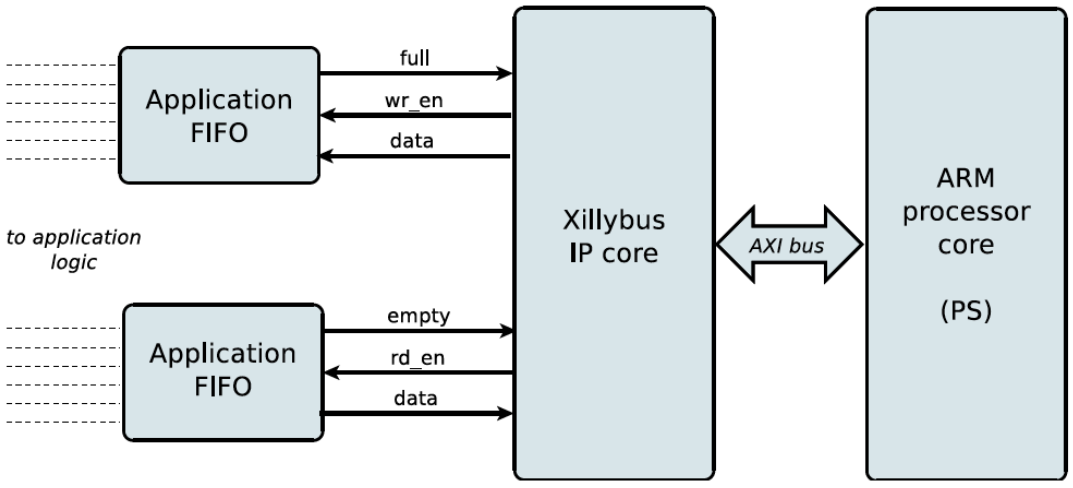

Figure 3.3: Xillybus overview[31]

3.3 FPGA reconfiguration workflow

To demonstrate the considerations encountered in the typical FPGA workflow, we walk through the implementation of a typical application: computation of the dot product of two vectors.

3.3.1 Typical Application: Dot Product of Vectors

Dot product (or scalar product) is an operation that takes two equal-length vector of numbers and returns a single number. Algebraically, it is defined as the sum of the product of the corresponding entries of the two sequences of numbers (Algorithm 1). Geometrically, it is the length of one vector projected on the other. Dot product, important in many scientific applications, is a good candidate for hardware acceleration.

Algorithm 1 Dot Product

Require: Input n > 0, A and B non empty

1: $i \leftarrow 0$
2: $result \leftarrow 0$
3: **while** i $<$ n **do**
4: $\quad result \leftarrow result + A[i] \times B[i]$
5: $\quad i \leftarrow i + 1$
6: **end while**
7: **return** *result*

3.3.2 Describing the Circuit

The first step towards using the Zynq PL is describing a circuit that will compute the target function. Xilinx supports the two most common *hardware description languages* (HDL), Verilog and VHDL. We chose to use VHDL for this project. Even though VHDL code may look similar to code from traditional software programming languages, there are important difference. VHDL is a parallel dataflow language, unlike sequential computing languages such as C and assembly code. While sequential language instructions must be interpreted by the CPU, VHDL code creates a defination file for an inherently parallel circuit that can be realized directly as a circuit or indirectly as an FPGA hardware.

```
1  int dot_product(int* A, int* B, int size){
2
3      int result;
4      int i = 0;
5
6      for(i = 0; i < size; i++){
7
8          //pass A[i] and B[i] to the PL
9          pass_args_to_PL(A[i],B[i],size);
10
11         //synchronize data communication
12         //and wait for the computation to complete
13         synchronize_and_wait();
14     }
15
16     //retrieved the result
17     retrieve_result(result);
18
19     return result;
20 }
```

Listing 3.1: Software invoking operation on hardware

```
1  -- arguments are stored as local signals
2  signal val1: std_logic_vector(31 Downto 0) := get_first_argument();
3  signal val2: std_logic_vector(31 Downto 0) := get_second_argument();
4  signal size: integer := to_integer(unsigned(get_third_argument()));
5
6  signal result: std_logic_vector(31 Downto 0);
7  signal count : integer := 0;
8  signal state : integer := computing;
9
10 -- perform computation every clock cycle
11 signal temp_data: std_logic_vector(31 Downto 0);
12 case state is
13   when computing =>
14     if (count /= size) then
15
16         temp_data <= multiply(val1, val2);
17         result <= result + temp_data;
18         state <= computing;
19         count <= count + 1;
20
21         --signal computation performed; synchronize
22         computation_performed();
23     else
24         state <= done;
25     end if;
26   when done =>
27     transfer_result_back(result);
28     state <= complete;
29  end case;
```

Listing 3.2: Hardware implementation in VHDL

To show how to perform dot product of vectors using this software-hardware hybrid architecture, we implemented Algorithm 1 in C and VHDL. These two implementations are shown in Listings 3.1 and 3.2, respectively.

The computation is initiated in the processing system (PS), with software passing required values to the hardware. The software then waits. Once the programmable logic (PL) gets the required values, the computation starts. Computation happens every clock cycle. Since the clocks are running at different speed on PS and PL, two computing partners must be synchronized. This process repeats until all the entries of the vectors have been consumed. The PL then sends the result back to the software, and the computation is complete.

3.3.3 Simulation

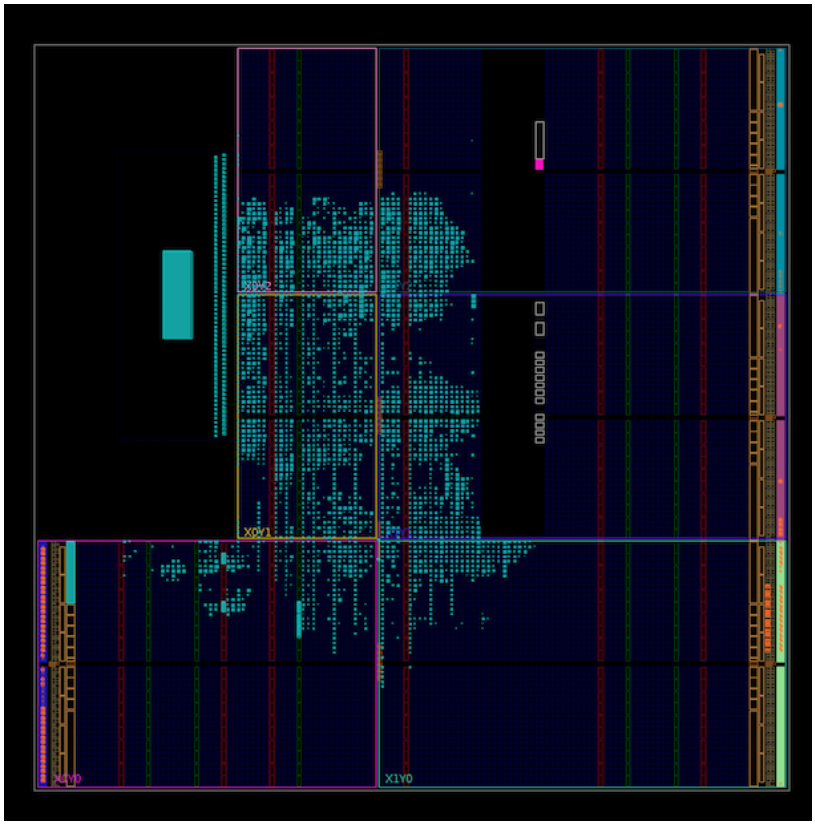

Figure 3.4: Implemented circuit diagram

Since producing a hardware circuit is a lengthy process, *simulation* is a crucial tool for designing any hardware efficiently in an FPGA. Testing a VHDL circuit is significantly more complex than testing a software application. There are various level of granularity at which

a circuit can be simulated (eg, high level behavioral correctness to estimating propagation delays) and a VHDL *testbench* created for simulation must accurately mimic the hardware environment. Instead of simply calling a function with few different test inputs, a designer must define and provide a clocking mechanism and interfaces between the circuit being tested and the testing unit.

The next step is inserting any new *intellectual property* (IP) blocks. To use the newly created IP core, it must be interconnected with other hardware, which effectively lays out a floor plan. This involves importing other Xilinx IPs, including the IP for the ARM PS, and connecting the different pieces of IP correctly.

3.3.4 Synthesis and Implementation

Once the block diagram is complete and all interconnects have been managed correctly, it is synthesized and implemented. Unlike software compilation, which usually takes a few seconds, Vivado's synthesis generally take a few minutes to run. This makes turnaround time to updating an IP core extremely time consuming, as even minor changes require a significant amount of time to implement. Synthesis and implementation output many reports, some of which detail the resource utilization of the IP cores, and predicted power consumption by the implemented circuit. A picture of hardware implementation of the design is shown in Figure 3.4. Finally, bitstream is generated for the implemented design. The bitstream file augments the system boot file and is loaded by the first stage boot loader to initialize the FPGA before the processor is booted. Once installed, the hardware is available through Xillybus device file.

3.4 Summary

Even though Zynq is a great system to build a tightly-coupled coprocessor for a GPP, the process of programing the system is very much involved. We believe that complexity of this process represents a significant "barrier-to-entry" for new applications. This is unfortunate, given the great potential of these systems. In the next chapter, we describe an IP core that, at a high level, can be reconfigured or reprogrammed very easily. We believe this approach of targeting a reconfigurable one-time-programmed co-processor represents a happy medium between dedicated ASIC design and user-driven FPGA design as it combines the flexibility and efficiency of both.

4. Faux-Vector Processor

In-spite of the complex programming model, the concept and benefits of an FPGA-based co-processor is very promising as it combines favourable characteristics of GPP and ASIC designs. In this section, we propose a FPGA-based vector reconfigurable co-processor. Along with the design and implementation details of the co-processor, we also provide some example applications that make use of the co-processor.

Previous research suggests that FPGA-based co-processors can provide significant performance improvement over a GPP alone. However, FPGA flexibility and efficiency comes at a significant workflow-cost. The devices are complex (Zynq's 1863 page manual [30]); the learning curve for VHDL is steep; and the configuration tool is buggy and poorly documented. Still, FPGAs remain popular devices supporting soft processors used in embedded systems. Soft processors are HDL-specified processors that can be configured in various ways supporting varying performance and resource utilization. The key benefit of using FPGAs for soft processors is that they can achieve high performance with reduced development effort to the user once they are designed. As a primary goal to this work, we have designed a soft vector processor called the Faux-Vector Processor (FVP).

In this new power-conscious era, efforts like the Conservation Core project from UCSD [27] have demonstrated a new way of designing power-efficient chips by configuring the excess transistors on the chip as power efficient hardware for specific application. In this work, we replace ASIC-like static core with a FPGA-based reconfigurable core, the FVP. This vector processor is optimized for power efficiency rather than speed. In a traditional GPP, a significant percent of power consumption comes from interpreting instructions. Vector processors perform entire loops as a single instruction so they can significantly reduce the power associated with instruction interpretation. We leverage this aspect of vector processor design to implement a single lane vector processor to realize the potential of performing computation with less overall power. The single lane vector processor executes operations sequentially rather than in parallel, hence the name *Faux* Vector Processor.

4.1 FVP Architectural Overview

The FVP is a *single-instruction-multiple-data* (SIMD) array of *virtual processors* (VPs) embedded on a Zynq processor. The number of VPs is the same as the *vector length* (VL). All VPs execute the same operation specified by a single vector instruction. The instruction set in this architecture borrows heavily from the VIRAM instruction set [21], which is designed as a vector extension to the MIPS-IV instruction set. A few instructions are borrowed from VESPA's ISA [33]. Operations however are performed sequentially rather than in parallel; the processor's focus is the development of power-efficiency without reduction of performance.

4.1.1 Interface

`NLane` and `MVL` are fixed for the processor. They control the number of parallel vector lanes and functional units that are logically available in the processor, and the maximum length of the vectors that can be stored in the processor's vector register file, respectively. `VPW` and `MemMinWidth` control the data width of the VPs, and the minimum data width that can be accessed by vector memory instructions, respectively. Table 4.1 shows the list of parameters for the processor, their descriptions, and possible values.

Table 4.1: List of parameters for the Faux Vector Processor

Parameter	Description	Range of values	Type
NLane	Number of lanes	1	Fixed
MVL	Maxumum vector length	64	Fixed
VPW	Processor data width (in bits)	8,16,32	Variable
VL	Vector Length	1-64	Variable
MemWidth	Memory interface width (bits)	32,64	Variable
MemMinWidth	Minimum accessible data width in memory	8,16,32	Variable

The architecture defines sixty-four vector registers, and thirty-two 32-bit scalar registers. Vector-scalar instructions and certain memory operations require vector register and scalar register operands. Scalar register values can be transferred to and from vector registers or vector control registers using the `vext`, `vins`, `vmstc`, `vmcts` instructions.

Further, the architecture defines thirty-two vector flag registers. The flag registers are written to by comparison instructions and are operated on by flag logical instructions. The

Table 4.2: List of vector flag registers

Hardware Name	Software Name	Contents
$vf0	vfmask0	Primary mask
$vf1	vfmask1	Secondary mask
$vf2	VF0	General purpose
...	...	...
$vf31	VF29	General purpose

`vector masks` are stored in the first two vector flag registers. Almost all instructions in the instruction set support conditional execution using a vector mask, specified by a mask bit. Table 4.2 shows a complete list of flag registers.

The architecture also defines sixty-four control registers. These registers are responsible for controlling the communication of important information between the host and the co-processor. Table 4.3 shows a complete list of control registers and their use.

Table 4.3: List of control registers

Hardware Name	Software Name	Contents
$vc0	VL	Vector length
$vc1	VPW	Virtual processor width
$vc2	VINDEX	Element index for insert (vins) and extract (vext)
$vc32	vstride0	Stride register 0
...	...	...
$vc39	vstride7	Stride register 7
$vc40	vinc0	Auto-increment Register 0
...	...	...
$vc47	vinc7	Auto-increment Register 7
$vc48	vbase0	Base register 0
...	...	...
$vc63	vbase7	Base register 7

4.1.2 Instruction Set Architecture

The following section describes, in detail, the instruction set of the FVP.

Data Types

The data widths supported by the processor are 32-bit words, 16-bit halfwords, and 8-bit bytes, and only unsigned data types.

Addressing Modes

The instruction set supports two vector addressing modes:

1. Unit stride access, when values are found in adjacent locations.
2. Constant stride access, when logically adjacent values are separated by a constant number of bytes.

Flag Register Use

Almost all instruction can specify one of two vector mask registers in the opcode to use as an execution mask. By default, `vfmask0` is used as the vector mask. Writing a value of 0 into the mask register will cause the VP to be disabled for operations that use the mask. Some instructions, such as flag logical operations, are not maskable.

Instructions

Table 4.4 describes the possible qualifiers in the assembly code describing each instruction.

Table 4.4: Instruction qualifiers for opcode op

Qualifier	Meaning	Description
op.vv op.vs	Vector-vector Scalar-vector	Vector arithmetic instructions may take one source operand from a scalar register. A vector-vector operation takes two two vector source operands from the vector register file; a vector-scalar operation takes second operand from a scalar register file.
op.b op.h op.w	1B Byte 2B Halfword 4B Word	All vector memory instructions need to specify the width of integer data, which may be 1, 2, or 4 bytes.
op.1	vfmask1 as the mask	The vector mask is taken from vfmask0 by default. This qualifier selects vfmask1 as the vector mask.

The instruction set includes the following categories of instructions:

1. Vector Arithmetic Instructions, for arithmetic operations on vectors.
2. Vector Logical Instructions, for comparison of vectors.
3. Vector Flag Processing Instructions, for explicitly loading and storing mask values.
4. Vector Processing Instructions
5. Memory instructions, for loading and storing vectors.

Table 4.5: Vector arithmetic instructions

Name	Mnemonic	Syntax	Summary
Absolute Value	vabs	.vv[.1] vD, vA	Each unmasked VP writes into vD the absolute value of vA.
Add	vadd	.vv[.1] vD, vA, vB .vs[.1] vD, vA, rS	Each unmasked VP writes into vD the unsigned integer sum of vA and vB or rS.
Subtract	vsub	.vv[.1] vD, vA, vB .vs[.1] vD, vA, rS	Each unmasked VP writes into vD the unsigned integer result of vA minus vB or rS.
Multiply Low	mult	.vv[.1] vD, vA, vB .vs[.1] vD, vA, rS	Each unmasked VP writes into vD the lower half of unsigned integer result of vA times vB or rS.
Shift Right Logical	vsra	.vv[.1] vD, vA, vB .vs[.1] vD, vA, rS	Each unmasked VP writes into vD the result of logical right shifting vA by vB or rS.
Shift Left Logical	vsrl	.vv[.1] vD, vA, vB .vs[.1] vD, vA, rS	Each unmasked VP writes into vD the result of logical left shifting vA by vB or rS.
Minimum	vmin	.vv[.1] vD, vA, vB .vs[.1] vD, vA, rS	Each unmasked VP writes into vD the minimum of vA and vB or rS.
Maximum	vmax	.vv[.1] vD, vA, vB .vs[.1] vD, vA, rS	Each unmasked VP writes into vD the maximum of vA and vB or rS.
Compare Less Than Compare Less than Equal	vcmplt vcmplte	.vv[.1] vF, vA, vB .vs[.1] vF, vA, rS	Each unmasked VP writes into vF the boolean result of comparing vA and vB or rS.
Compare Equal Compare Not Equal	vcmpe vcmpne	.vv[.1] vF, vA, vB .vs[.1] vF, vA, rS	Each unmasked VP writes into vF the boolean result of comparing vA and vB/rS.
Multiply Accumulate	vmac	.vv[.1] vD, vA, vB .vs[.1] vD, vA, rS	Each unmasked VP calculates the product of vA and vB or rS. The products of the vector elements are added, and the sum is written to an internal accumulator register.
Copy from Accumulator	vccacc	vD	The internal accumulator register is written to the first VP of vD, and zeroed.

Table 4.6: Vector logical instructions

Name	Mnemonic	Syntax	Summary
And	vand	.vv[.1] vD, vA, vB .vs[.1] vD, vA, rS	Each unmasked VP writes into vD the logical AND of vA and vB/rS.
Or	vor	.vv[.1] vD, vA, vB .vs[.1] vD, vA, rS	Each unmasked VP writes into vD the logical OR of vA and vB/rS.
Xor	vxor	.vv[.1] vD, vA, vB .vs[.1] vD, vA, rS	Each unmasked VP writes into vD the logical XOR of vA and vB/rS.
Nor	vnor	.vv[.1] vD, vA, vB .vs[.1] vD, vA, rS	Each unmasked VP writes into vD the logical NOR of vA and vB/rS.

Table 4.7: Move instructions

Name	Mnemonic	Syntax	Summary
Move Scalar to Control	vmstc	vc, rS	Content of rS is copied to vc.
Move Control to Scalar	vmcts	rS, vc	Content of vc is copied to rS.
Move to Scalar	mov	rS, value	value is copied to rS.

Table 4.8: Vector flag processing instructions

Name	Mnemonic	Syntax	Summary
And	vfand	.vv vFD, vFA, vFB .vs vFD, vFA, rS	Each VP writes into vFD the logical AND of vFA and vFB/rS.
Or	vfor	.vv vFD, vFA, vFB .vs vFD, vFA, rS	Each VP writes into vFD the logical OR of vFA and vFB/rS.
Xor	vfxor	.vv vFD, vFA, vFB .vs vFD, vFA, rS	Each unmasked VP writes into vFD the logical XOR of vA and vB/rS.
Nor	vnor	.vv vFD, vFA, vFB .vs vFD, vFA, rS	Each unmasked VP writes into vFD the logical NOR of vFA and vFB/rS.
Clear	vfclr	vFD	Each VP writes zero into vFD.
Set	vfset	vFD	Each VP writes one into vFD.
Population Count	vfpop	rD, vF	The count of non zero values of vF is written to rD.

Table 4.9: Memory instructions

Name	Mnemonic	Syntax	Summary
Unit Stride Load	vld	{.*b.h.w*}[.1] vD, vbase, [vinc]	The VPs perform a continuous vector load into vD. The signed increment vinc is added to vbase as side effect. The width of each element is derived from VPW.
Unit Stride Store	vst	{.*b.h.w*}[.1] vS, vbase, [vinc]	The VPs perform a continuous vector store from vS. The signed increment vinc is added to vbase as side effect. The width of each element is derived from VPW.
Constant Stride Load	vlds	{.*b.h.w*}[.1] vD, vbase, vstride, [vinc]	The VPs perform a stride vector load into vD. The signed increment vinc is added to vbase as side effect. The width of each element is derived from VPW.
Constant Stride Store	vsts	{.*b.h.w*}[.1] vS, vbase, vstride, [vinc]	The VPs perform a stride vector from vS. The signed increment vinc is added to vbase as side effect. The width of each element is derived from VPW.
Vector Flag Flag load	vfld	vFD, vbase	The VPs perform a vector flag load to vFD.
Vector Flag Flag Store	vfst	vFA, vbase	The VPs perform a vector flag store from vFA.

Table 4.10: Vector processing instructions

Name	Mnemonic	Syntax	Summary
Vector Shift	veshift	vD, vA, dir	The contents of vA are shifted up by one element in the specified direction (left or right), and the result is written to vD.
Merge	vmerge	.vv[.1] vD, vA, vB .vs[.1] vD, vA, rS	Each VP copies into vD either vA if the mask is 1, or vB/rS if the mask is 0.
Vector Extract	vext	.sv vS, vA	The contents of a VP in vA is copied into vS. `vindex` specifies the VP index.
Vector Insert	vins	.vs vD, vS	The contents of vS are written into vD at location `vindex`.

Table 4.5 shows the list of arithmetic instructions. Table 4.6 shows the logical instruction. Table 4.7 shows the move instructions. Table 4.8 shows the flag processing instructions. Table 4.9 shows the memory instructions. Finally, Table 4.10 shows the vector processing instructions. All the operations are masked except for all the vector flag operation, veshift, vccacc, flag load and store, and vector insert and extract instructions.

4.1.3 FPGA Implementation

The basic model for the FVP is a state machine that performs fetch, decode, or execution of instruction on every clock cycle. The block diagram of the architecture is shown in figure 4.1. The architecture consists of a scalar ARM core, a vector processing unit, and a memory interface unit. The memory interface unit acts as a shared memory and helps the scalar core and the vector processing unit communicate. In this section, we describe the memory interface unit.

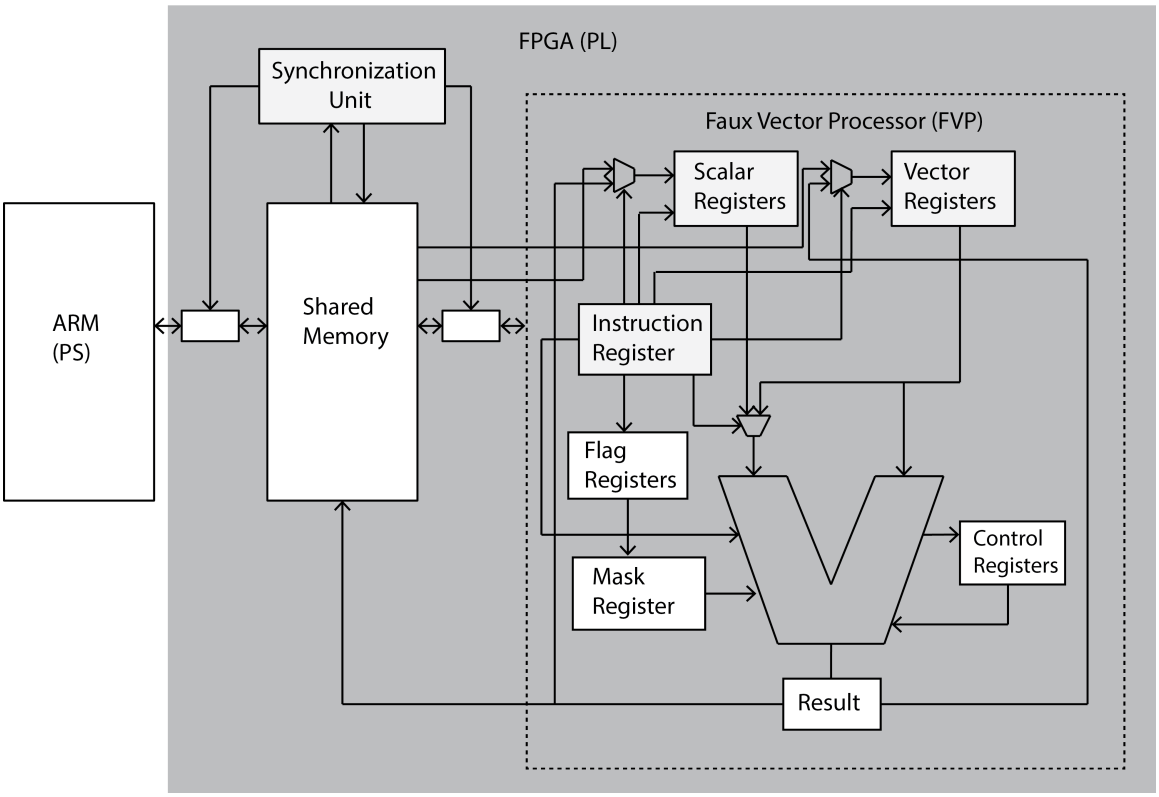

Figure 4.1: Block diagram of FVP architecture.

The memory interface sits between the scalar ARM processor on the PS and the vector processing unit on PL. It is implemented using the Xillybus Lite. Figure 4.2 shows how the

shared memory is used. When the scalar processor is ready to execute an instruction on the vector processor, it loads the instruction into the shared memory's instruction register. After the instruction is loaded, the scalar core updates the current instruction ID - - an arbitrary value - - into the shared memory. While the current instruction ID and completed instruction ID differ, the FVP fetches the instruction from the shared memory, decodes it instantly, and then executes it in the next few cycles. Finally, after writing the results back, the vector processing unit signals completion by coping the current instruction ID into the shared completed instruction ID register. This logically transfers control back to the scalar core. This mechanism allows us to synchronize computation. This process repeats every time the scalar core wants to execute an instruction on the vector processing unit.

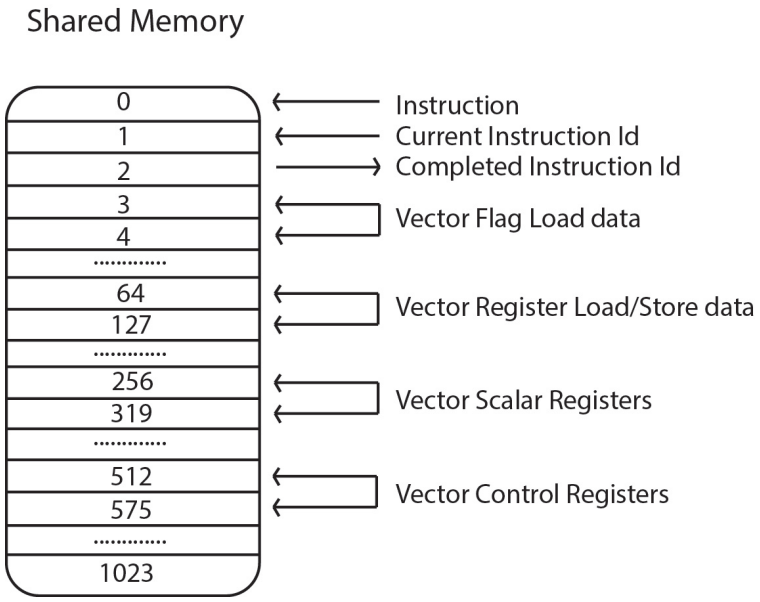

Figure 4.2: Block Diagram of Memory Interface Unit.

Besides instruction transfer and synchronization, the shared memory also acts as register file. All the scalar registers and control registers of the vector processor are located in this shared memory to allow for their easy access from the scalar core. Since the vector processor and the ARM processor do not share a common address space, the shared memory is also used as a temporary storage space to move values between the vector processor and the scalar core during load and store instructions.

4.2 Programming the FVP from Processing System

In this section, we will give a basic outline of the interface to interact with the FVP. When a programmer wants to execute some operation, there are two possible paths: to execute the operation on the ARM processor, running the Linux operation system, or to make use of the vector processing unit. To execute an instruction on the vector processing unit, the user uses library calls written in C. These library calls are like any ordinary procedure calls and they hide details regarding instruction execution and synchronization. Typical library calls are shown in listing 4.1. Therefore, to perform any computation, the user simply can make these library calls in the middle of their program after setting parameters like `VL` and `VPW`.

```
void vld(int dest, int src1, int inc, int mask);
void vlds(int dest, int src1, int stride, int inc, int mask);
void vst(int src, int base, int inc, int mask);
void vsts(int src, int base, int stride,int inc, int mask);
void vadd(int dest, int src1, int src2 ,int mask);
void vabs(int dest, int src1, int mask);
void vmul(int dest, int src1, int src2, int mask);
void vand(int dest, int src1, int src2, int mask);
void vor(int dest, int src1 , int src2, int mask);
void vnor(int dest, int src1, int src2, int mask);
void vmac(int src1, int src2, int mask);
void vccacc(int dest);
void veshift(int dest, int dir);
void vfld(int dest,int64_t value);
void vfand(int dest, int src1, int src2);
void vfor(int dest, int src1, int src2);
void vfxor(int dest, int src1, int src2);
void vfnor(int dest, int src1, int src2);
void vfclr(int dest);
void vfset(int dest);
void vmin(int dest,int src1, int src2, int mask);
void vmax(int dest,int src1, int src2, int mask);
```

Listing 4.1: Few example library calls for FVP

Rather than using the library calls, a vectorizing compiler could be used to target our FVP. Even though our tools currently do not include a vectorizing compiler, we are confident that this support could be added later. We discuss this possibility in Chapter 6.

4.2.1 Design Examples

In this section, five benchmarks, representative of common applications are chosen to demonstrate the ease of use and advantages of the FVP. For each of the examples below, we present the representation in C, and equivalent code using our library calls.

Matrix Multiplication

Matrix Multiplication is a very popular operation in mathematics with wide range of applications. The code in Listing 4.2 shows matrix multiplication code in C, and the code in Listing 4.3 shows the library call equivalent of the same C code. In the library call version, one of the dimensions is handled by vectoring (removing) the inner loop.

```
1  void matrix_mul_c(int ib[n][n], int ic[n][n], int result[n][n], int
       n){
2       int i,j,k,sum;
3       for(i = 0; i < n; i++){
4           for (j = 0; j < n; j++){
5               sum = 0;
6               for (k = 0; k < n; k++) {
7                   sum += ib[i][k]*ic[k][j];
8               }
9               result[i][j] = sum;
10          }
11      }
12 }
```

Listing 4.2: Matrix multiplication in C

```
1  void matrix_mul_lib(int ib[n][n], int ic[n][n], int result[n][n],
       int n){
2
3       vmstc(VL,n);
4       vmstc(VPW,4);        // width of the data in bytes
5
6       vmstc(STRIDE1,n);    // row width
7       vmstc(STRIDE2,1);
8       vmstc(INC1,1);
9       vmstc(INC2,n);
10
11      vmstc(BASE0,result);
12      vmstc(BASE1,ib);
13      vmstc(BASE2,ic);
14
15      int i,j;
16      for(i=0;i<n;i++){
17        vld(VR2,BASE1,INC2,vfmask0);
18        vmstc(BASE2, &ic);
19        for(j=0; j<n;j++){
20          vlds(VR1,BASE2,STRIDE1,INC1,vfmask0);
21          vmac(VR2,VR1,vfmask0);
22          vccacc(VR3);
23          veshift(VR3,LEFT);
24        }
25        vsts(VR3,BASE0,STRIDE2,INC2,vfmask0);
26      }
27 }
```

Listing 4.3: Matrix multiplication in Library Calls

Initially, vector length, vector processor width (width of the data in bytes), and various stride and increment values are set using `vmstc` instruction. Inside the outer loop, in each iteration, a row of matrix `ia` is loaded to `VR2`. Inside the inner loop, a column of matrix `ic` is loaded to `VR1`. The instruction `vmac` then computes the accumulated sum of the product of register `VR2` and `VR1`. Instruction `vccacc` stores this result to the first VP of `VR3`, and instruction `veshift` shifts the contents of `VR3` to the left by one element. After the inner loop terminates, the row of n elements of the result matrix is ready to be retrieved. This process repeats for each row in the matrix `ib`. At the end, the result of matrix multiplication is in the matrix `result`.

4.2.1.1 SAXPY

SAXPY stands for "Single-Precision A·X Plus Y". It is a function in the standard Basic Linear Algebra Subroutines (BLAS) library. SAXPY is a combination of scalar multiplication and vector addition, and is a very useful operation in linear algebra and other related fields. It takes as input two vectors `X` and `Y` with n elements each, and a scalar value `A`. It multiplies each element `X[i]` by `A` and adds the value to `Y[i]` into the `result`. A simple C implementation is shown in Listing 4.4.

```
1 void saxpy_c(int * X, int * Y, int * result, int A, int n){
2     int i;
3     for (i = 0; i < n; i++){
4         result[i] = A*X[i] + Y[i];
5     }
6 }
```

Listing 4.4: SAXPY in C

```
1  void saxpy_lib(int * X, int * Y, int * result, int A, int n){
2
3      vmstc(VL,n);
4      vmstc(VPW,4);      \\ width of the data in bytes
5
6      vmstc(BASE1,X);
7      vmstc(BASE2,Y);
8      vmstc(BASE3,result);
9      vmstc(INC0,0)
10
11     mov(VS1,A);
12     vld(VR2,BASE1,INC0,vfmask0);
13     vld(VR3,BASE2,INC0,vfmask0);
14     vmul(VR1,VR2,VS1,vfmask0);
15     vadd(VR4,VR1,VR3,vfmask0)
16     vst(VR4,BASE3,INC0,vfmask0);
17 }
```

Listing 4.5: SAXPY in library calls

Our library call version of SAXPY is shown in Listing 4.5. Initially, `VL`, `VPW`, and base addresses are set using the `vmstc` instruction. Then `VR2` and `VR3` are loaded with the contents of vectors `X` and `Y` respectively. Similarly, a scalar register is also loaded with the value of constant `A`. Instruction `vmul` multiplies each element of vector `X` with constant `A`, and `vadd` adds the result of this multiplication with vector `Y`. The final result is stored back in vector `result`.

FIR Filter

In signal processing, a *finite impulse response* (FIR) filter is a filter that measures the weighted average of signals of finite length. FIR filter can be used to implement almost any sort of frequency response digitally. For a discrete-time FIR filter of order N, each value of the output sequence is a weighted sum of the most recent input values as described below.

$$\begin{aligned} y[n] &= b_0 x[n] + b_1 x[n-1] + ... + b_N x[n-N] \\ &= \sum_{i=0}^{N} b_i \times x[n-i] \end{aligned}$$

$x[n]$ is the input signal, $y[n]$ is the output signal, N is the filter order, b_i is the value of the impulse response at the i^{th} instant for $0 \leq i \leq N$.

Listing 4.6 and 4.7 shows FIR filter algorithm written in C and library call implementation, respectively for `n`-order FIR filter.

```
1  void filter_c(int * b, int n){
2
3    int i,y;
4    int x[n];
5    for (i = 0; i < n; i++){
6      x[i] = 0;
7    }
8
9    while (1){
10     for (i = n-1; i>0;i--){
11       x[i] = x[i-1];
12     }
13     scanf("%d",&x[0]);
14     y = 0;
15
16     for (i = 0; i<n; i++){
17       y += x[i] * b[i];
18     }
19     printf("%d\n",y);
20   }
```

```
21 }
```

Listing 4.6: FIR filter in C

```
1
2  void filter_lib(int * b, int n) {
3
4    vmstc(VL,n);
5    vmstc(VPW,4);
6    vmstc(VINDEX,0);
7
8    int x[n];
9    int i,y;
10   for (i = 0; i < n; i++){
11     x[i] = 0;
12   }
13
14   vmstc(BASE1,x);
15   vmstc(BASE2,b);
16   vmstc(INC0,0);
17
18   vld(VR0,BASE1,INC0,vfmask0);
19   vld(VR1,BASE2,INC0,vfmask0);
20
21   while (1){
22     veshift(VR0,RIGHT);
23     scanf("%d\n",&x[0]);
24     mov(VS0,x[0]);
25     vins(VR0,VS0);
26     vmac(VR0,VR1,vfmask0);
27     vcacc(VR2);
28     vext(VS0,VR2);
29     mov(&y,VS0);
30     printf("%d\n",y);
31   }
32 }
```

Listing 4.7: FIR filter in library Calls

Initially vector `x` is initialized with size `n` then loaded to `VR0`. Similarly, `b` is loaded to vector `VR1`. When a new value is read using `scanf`, `VR0` is rotated right by one element and the new value is inserted to location 0 of `VR0` by using `vins` instruction. This essentially drops the last N^{th} element from the input signal. Next, multiply accumulate operation is performed on registers `VR0` and `VR1` to produce the result.

String Comparison

String Comparison is another very popular loop that can be vectorized very easily. This application is partly picked to demonstrate the use of vector flags in our library calls.

Listing 4.8 shows a simple implementation of string comparison using character arrays, and Listing 4.9 shows corresponding library call implementation.

```
1 int string_cmp_c(char * srt1, char* str2, int n){
2     int i;
3     for( i = 0; i< n; i++){
4         if (str1[i] != str2[i]){
5             return 0;
6         }
7     }
8     return 1;
9 }
```

Listing 4.8: String comparison in C

The library call version is very straightforward to follow. Two vectors corresponding to the character arrays of two strings are loaded to vector registers after setting up the initial values like `VL`,`VPW`, etc. Next, the two vector registers are compared and the result is stored in a flag register. In this example, equal is used as a comparator. The instruction sets the flag for every VP for which the condition is met. Finally, with the help of instruction `vfpop`, total number of flags sets is counted. If there are no flags set then the two strings do not pass the comparison otherwise they do.

```
1  int string_cmp_lib(char * str1, char * str2, int n){
2
3      vmstc(VL,n);
4      vmstc(VPW,1);
5
6      vmstc(BASE1,str1);
7      vmstc(BASE2,str2);
8      vmstc(INC0,0);
9
10     vld(VR1,BASE1,INC0,vfmask0);
11     vld(VR2,BASE2,INC0,vfmask0);
12     vcmpe(VF1,VR1,VR2,vfmask0);
13     vfpop(VF1,VS0);
14
15     int result;
16     mov(&result,VS0);
17
18     return result == n;
19 }
```

Listing 4.9: String comparison in library calls

Compare and Exchange

Final benchmark to demonstrate the use of our library call is compare and exchange. Compare and exchange is a very common step in many sorting algorithms like merge sort, quick

sort, etc. The application also demostrates the use of flag registers. Listing 4.10 shows a simple compare and exchange algorithm written in C.

```
1 void cmp_exc_c(int * a, int * b, int n){
2     int i;
3     for(i = 0;i< n; i++){
4         if (compare(a[i],b[i])>0){
5             swap(&a[i],&b[i]);
6         }
7     }
8 }
```

Listing 4.10: Compare and exchange in C

```
1  void cmp_exc_lib(int * a, int * b, int n){
2
3      vmstc(VL,n);
4      vmstc(VPW,4);        // size of the data in bytes
5
6      vmstc(BASE1,a);
7      vmstc(BASE2,b);
8      vmstc(INC0,0);
9
10     vld(VR2,BASE1,INC0,vfmask0);
11     vld(VR3,BASE2,INC0,vfmask0);
12     cmplt(vfmask1,VR2,VR3,vfmask0);
13
14     //swap based on flag
15     vadd(VR2,VR2,VR3,vfmask1);
16     vsub(VR3,VR2,VR3,vfmask1);
17     vsub(VR2,VR2,VR3,vfmask1);
18
19     vst(VR2,BASE1,INC0,vfmask0);
20     vst(VR3,BASE2,INC0,vfmask0);
21 }
```

Listing 4.11: Compare and exchange in library calls

Listing 4.11 shows the same algorithm written in terms of our library calls. After setting up necessary control registers, the data is loaded to vector registers. Next, a comparison operation is performed, less than in our example. Like in string comparison, a vector flag is not set for every comparison that passes. Based on this vector flag, a simple swap is performed using masked `vadd` and `vsub` as described in Algorithm 2. Finally, the results are stored back after the swap.

4.3 Summary

The FVP and its support library as described in this section represents a first successful step towards large scale FPGA-based reconfigurable co-processor. With the help of library calls,

Algorithm 2 Swap using add and subtract

Require: Input a and b

1: $a \leftarrow a + b$
2: $b \leftarrow a - b$
3: $a \leftarrow a - b$

the architecture provides a level of abstraction which makes it possible for software engineers to make use of custom co-processors without having to deal with hardware directly. In the near future, system like ours will reduce the complexity of using hardware for software development so that it can reach the degree of convenience that software developers have long become used to. More importantly, the FPGA's reconfigurability gives this architecture the flexibility to modify and improve the design without any significant financial or technical ramifications. FPGA-based co-processor avoids the need to decide on a set of specialized units at chip design time. Rather, new or improved specialized units could be added to the chip at any time. At the same time, no chip resources are wasted for specialized functionality that a particular system installation may never actually need.

5. Faux-Vector Processor Performance Estimation

The current implementation of the FVP described in Chapter 4 is a first step towards creating a configurable co-processor tightly couple with a GPP. In this Chapter, we describe the efficiency, both in terms of performance and energy, of the design described in Chapter 4. Specifically, we describe the components of our infrastructure necessary to execute, verify, and evaluate instructions for the FVP.

5.1 Methodology

Along with our hardware implementation of FVP, we also implemented a software simulation of the the co-processor written in the C programming language. The reason behind the software simulation is to accurately compare the performance between implementing the same exact logic on hardware and software. All of the instructions for the vector processor were tested and verified both on hardware and software implementations of the FVP. Furthermore, we also compare the performance of implementing all of our benchmark programs described in Section 4.2.1 purely on the ARM processor and on the ARM processor with FVP as a tightly coupled co-processor. Finally, we begin analysis of the power consumed by the hardware implementation of the FVP.

5.2 Hardware Utilization

Figure 5.1 shows the estimated hardware resource utilization with and without the current implementation of the FVP on the Zynq device. A functional Zynq system without FVP core includes a VGA core to support VGA interface, two AXI buses, and Xillybus-lite core to help aid the communication between ARM (PS) and FVP (PL). We can see from the resource utilization table that the vector processor mainly consumes logic slices. As a result,

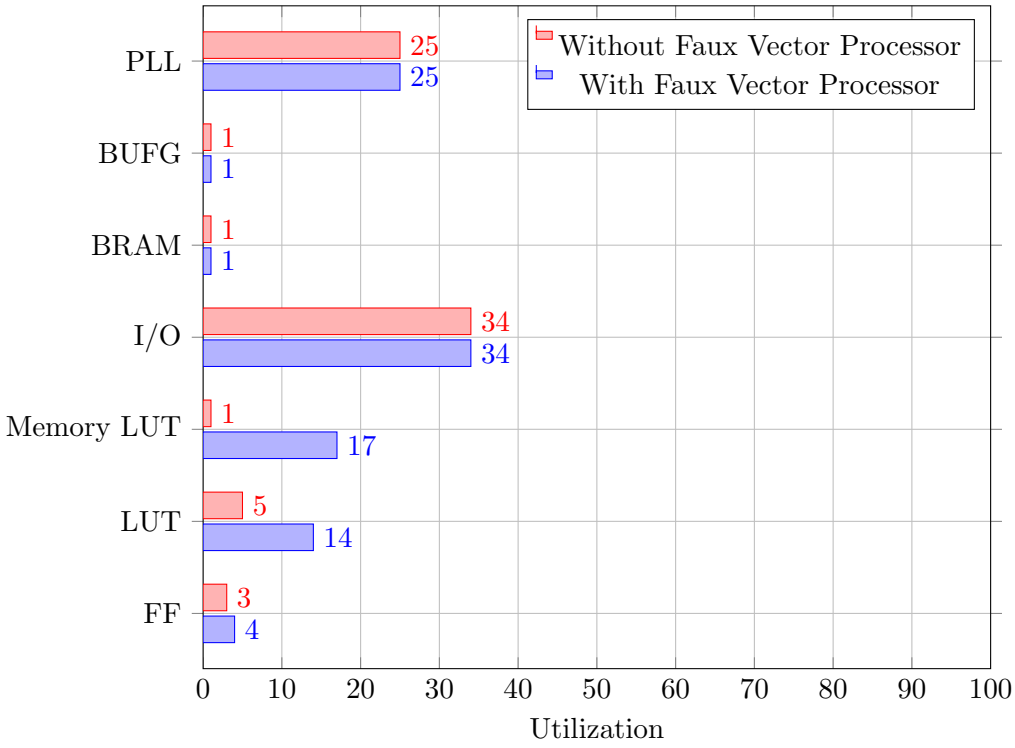

Figure 5.1: Resource utilization of hardware implementation with and without FVP.

the logic overhead is about 4% of FF, 14% of LUT, and 17% of Memory LUT. FF are flip-flops, registers that store machine state. LUT are lookup tables, hardware that supports implementation of custom logic. The co-processor design also utilizes a small percent of digital signal processing unit called DSP48 slice to support efficient multiplication.

As we can see from the graph, FVP is only responsible for a small fraction of the Zynq's resources. Hardware resources like PLL, BUFG, BRAM and IO are not utilized by the FVP and are mainly consumed by Xillybus architecture. We believe that the overall resource utilization can be further reduced if we replace Xillybus with our synchronization core.

5.3 Vector Performance

In this section, we measure the performance of executing instructions on the software versus the hardware implementation of the FVP. We wanted to measure the performance of implementing the same circuit on software and hardware as this would allow us to measure the relative efficiency of running the same program on hardware and software. To measure the execution time, each of the instruction is performed 10000 times and the best average time of these runs over 100 repetitions is recorded. The process is repeated for varying vector

lengths. Next, by fitting an appropriate line to the data, we are able to identify the overhead associated with starting a computation (indicated by y-intercept) and the marginal cost of performing operation on one more element (indicated by slope).

Figure 5.2 and Figure 5.3 shows the performance of executing vector load and store instruction on vectors of length 1 through 64. Table 5.1 shows the slope and y-intercept of the graphs from Figure 5.2 and Figure 5.3. As we can see from the graph, the software implementation for both load and store instruction is more efficient for smaller vector lengths. This is because the synchronization time consists of the majority of the execution time on vectors of smaller length. Synchronization time is the cost of starting an operation on the co-processor and is indicated by the y-intercept. However, the marginal cost of loading or unloading additional value is more efficient on the hardware implementation as shown by the slopes in Table 5.1.

Table 5.1: Load Store Instructions' Slope and Y-intercept

Instruction	Load(Hardware)	Load(Software)	Store(Hardware)	Store(Software)
Slope	266.7	319.9	258.1	380.6
Y-intercept	1148	716	1156	706

Figure 5.4 and Figure 5.5 show the performance of executing two arithmetic instructions: vector add and multiply, on vectors of length 1 through 64. The performance graphs for the arithmetic instructions is very similar to that of memory instructions. The software implementation is faster for smaller vectors while the hardware instruction is faster for larger vectors. Table 5.2 shows the slopes and y-intercepts of the graph shown in Figure 5.4 and Figure 5.5. The hardware implementation is more efficient for arithmetic instruction than for memory instruction as the marginal cost of add or multiply instruction on one more vector entry is significantly less than that of load or store instruction. Reading and writing values across PL and PS is significantly more expensive than to and from a register file.

Table 5.2: VMUL and VADD instructions' slope and y-intercept

Instruction	VADD(Hardware)	VADD(Software)	VMUL(Hardware)	VMUL(Software)
Slope	30.14	160.1	49.66	177.3
Y-intercept	1085	778	1101	812.5

Figure 5.6 and Figure 5.7 show the performance of executing two vector operations: vector

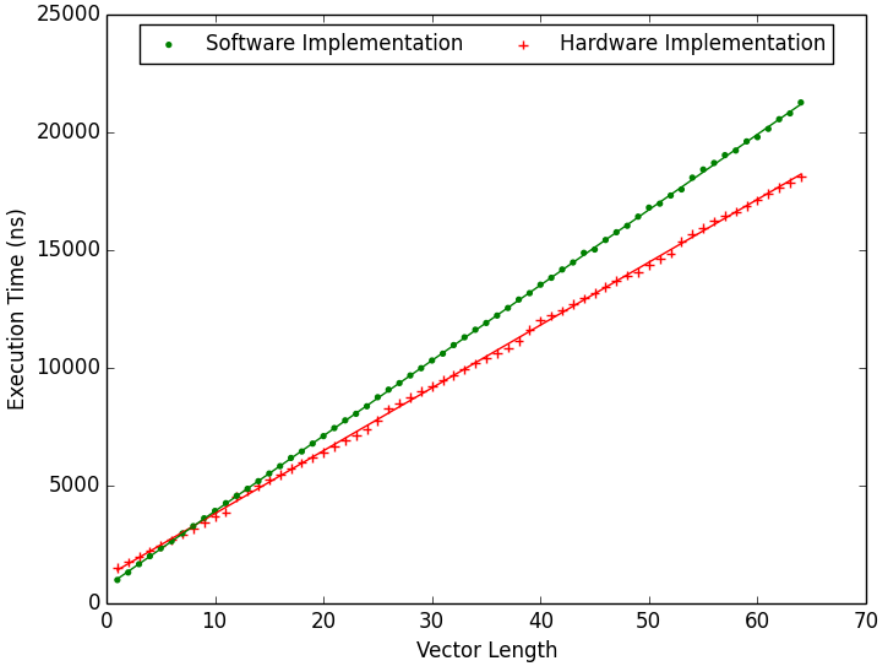

Figure 5.2: Performance of VLD instruction

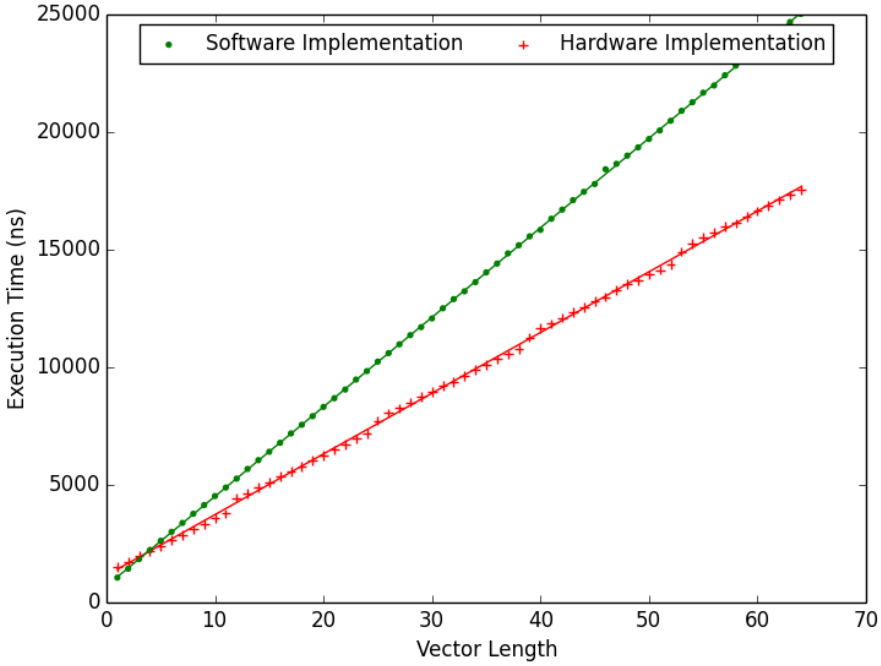

Figure 5.3: Performance of VST instruction

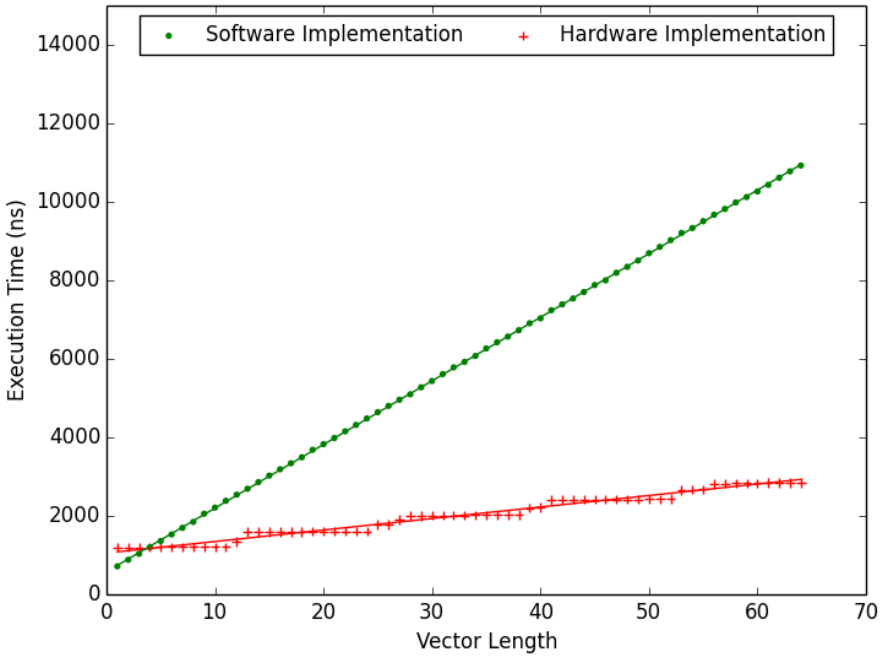

Figure 5.4: Performance of VADD instruction

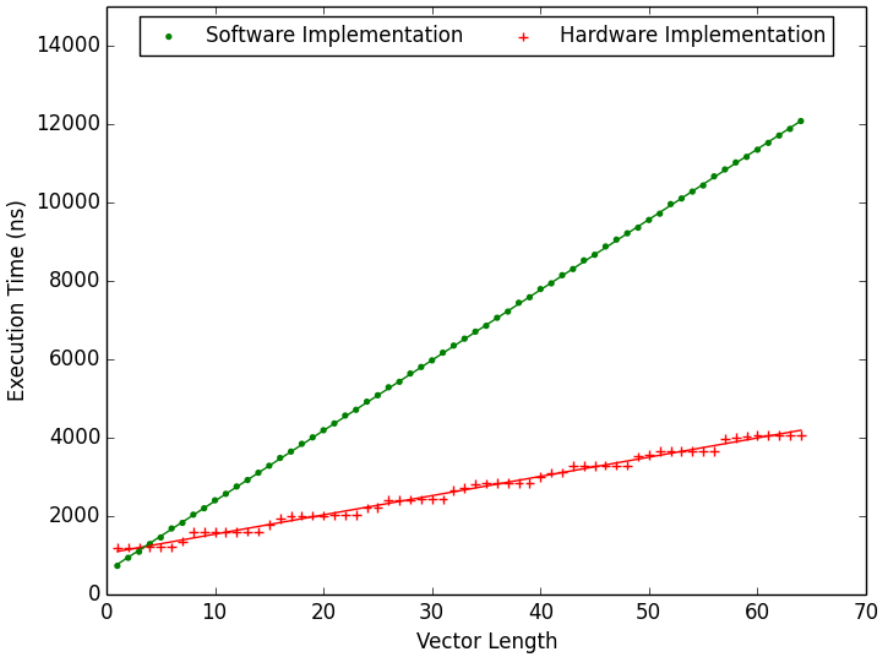

Figure 5.5: Performance of VMUL instruction

shift and multiply accumulate on vectors of length 1 through 64. The execution of the vector instructions is also faster on the hardware compared to the software version of the FVP. Like memory and arithmetic instructions, the performance gain of hardware implementation is only realized when the vectors become large as for smaller vectors the overhead of instruction synchronization is high. Table 5.3 shows the slopes and y-intercepts for the graphs in Figure 5.6 and Figure 5.7.

Table 5.3: VESHIFT and VMAC instructions' slope and y-intercept

Instruction	VESHIFT(Hardware)	VESHIFT(Software)	VMAC(Hardware)	VMAC(Software)
Slope	19.24	127.5	48.86	152.8
Y-intercept	1066	580.3	1055	568.3

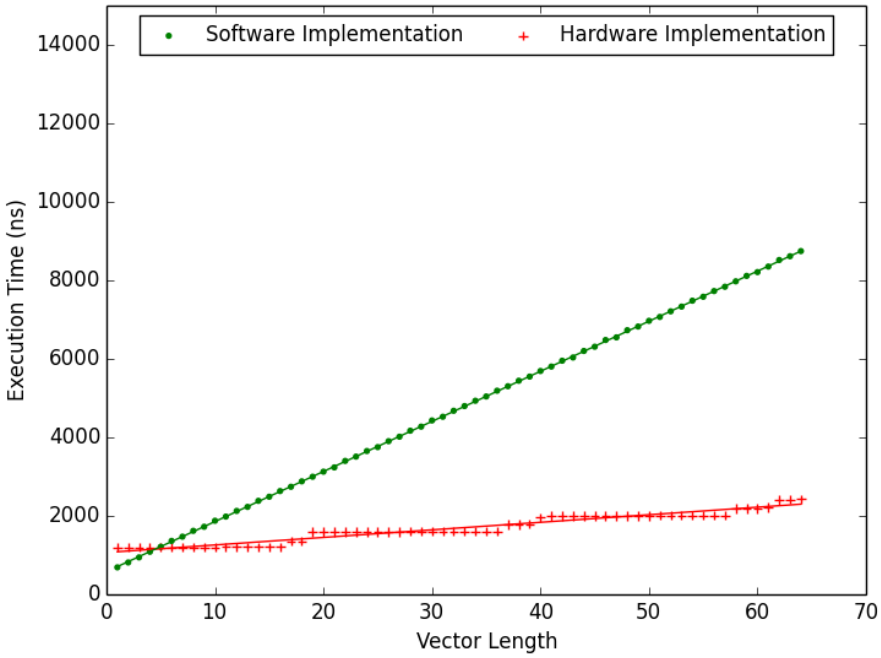

Figure 5.6: Performance of VESHIFT instruction

Figure 5.8 shows the performance of executing a vector flag operation on hardware vs software implementation of the FVP. Unlike other operations, the software implementation is significantly faster than the hardware implementation of the FVP. Flag operations are basically constant time operations and they do not depend on the vector length. As a result,

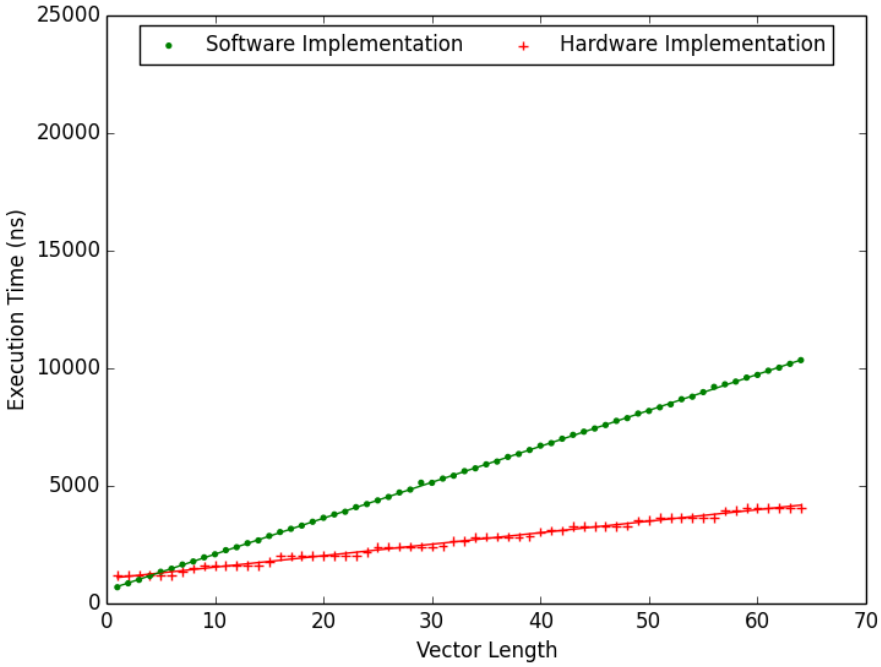

Figure 5.7: Performance of VMAC instruction

the execution time is dominated by the overhead of instruction synchronization. Table 5.4 shows the slope and y-intercept of the graph in Figure 5.8.

Table 5.4: VFAND instructions' slope and y-intercept

Instruction	VFAND(Hardware)	VFAND(Software)
Slope	0.1633	1124
Y-intercept	0.003012	648.7

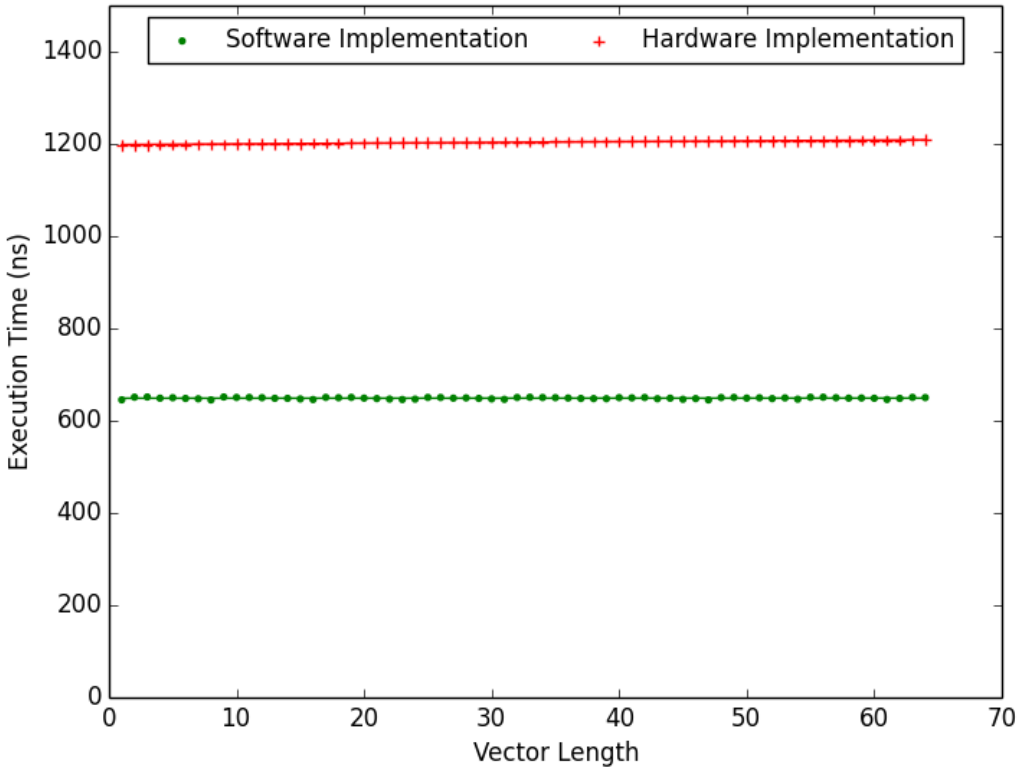

Figure 5.8: Performance of VFAND operation

The performance measurements of these instructions have shown that vectors of larger length give a better estimate of the efficiency of executing an instruction on hardware versus software implementation of the FVP. With smaller lengths, the overhead of instruction synchronization time dominates the execution time.

Finally, Table 5.5 summarizes the marginal cost and synchronization time for all the instructions in our instruction set. From the table, we can see that the only instructions whose execution is not dependent on the vector length are faster on software simulation of FVP, like flag operations. After paying the overhead cost of instruction synchronization, all the other operations are faster on the hardware implementation.

5.4 Benchmark Performance

In this section, we measure the performance of executing all of the benchmark programs described in Section 4.2.1 on our hybrid hardware-software architecture (with FVP as a co-processor) and purely on software. Figure 5.9, 5.10, 5.11, 5.12, 5.13 show the performance graph for matrix multiplication, SAXPY, FIR filter, compare and exchange, and string comparison, respectively.

As we can see from the graphs, all the benchmark programs perform better on pure software implementation than on the hybrid hardware-software system with FVP as co-processor. The hybrid architecture suffers heavily from the overhead of instruction synchronization before and after performing any useful computation. However, the marginal cost of performing operation of additional vector entry is significantly smaller for hardware implementation for all the benchmark programs except compare and exchange. As a result, we expect the hybrid architecture to eventually perform better than the pure software implementation. We believe that the vectors of length 64 are not large enough for this effect to be obvious. Particularly evident from SAXPY and FIR filter performance graphs, this effect is to be expected on larger vectors. For SAXPY, the slope of the hardware-software performance curve is 79 where as the slope of pure software performance cure is 109. If we extrapolate the graphs, the hybrid architecture will outperform pure software after vectors of length 72. Similarly, in case of FIR filter, the slope of the hardware-software performance graph is 77 while the slope of the pure software performance curve is 124. Hence, the hybrid implementation will outperform the pure software implementation after vector of length 112. In the case of compare and exchange, both the synchronization cost (y-intercept) and marginal cost (slope) is higher for performing the operations on the hybrid architecture than on pure software. We accept that not all applications are well suited for this architecture

Table 5.5: Software vs hardware performance for all instructions

Instructions	Marginal Cost of Operation		Instruction Synchronization Time	
	Hardware FVP	Software FVP	Hardware FVP	Software FVP
VADD	30.14	160.1	1085	788.2
VSUB	31.40	162.0	1100	750.1
VMUL	49.66	117.3	1101	812.5
VAND	31.21	161.3	1120	740.1
VABS	32.12	159.1	1150	690.0
VOR	33.10	164.2	1120	693.2
VNOR	32.10	152.2	1090	695.3
VXOR	32.29	162.1	1117	705.1
VSLL	38.10	170.2	1120	800.1
VRSL	39.20	171.4	1118	802.1
VFAND	0.1633	0.003132	1123	648.7
VFOR	0.1812	0.003052	1124	648.6
VFXOR	0.1932	0.003051	1124	648.5
VFNOR	0.2101	0.002998	1120	648.7
VFCLR	0.1601	0.003092	1120	648.7
VFSET	0.1601	0.003092	1121	648.5
VCMP_LT	41.20	178.2	1100	700.1
VCMP_LTE	42.10	180.6	1130	710.1
VCMP_E	40.60	181.2	1090	698.2
VCMP_NE	39.90	179.6	1098	702.1
VFPOP	0.1930	0.003101	1110	752.1
VMAX	33.10	172.1	1150	680.2
VMIN	32.90	170.6	1180	690.3
VESHIFT	19.24	127.5	1066	580.3
VMAC	48.86	152.8	1055	568.3
VLD	266.7	319.9	1148	716.3
VLDS	270.1	325.2	1180	720.0
VFLD	0.2130	0.00310	1160	690.9
VST	258.1	380.6	1156	706.1
VSTS	260.2	380.5	1165	720.1
VCACC	0.3120	0.003992	1150	710.2
VMERGE	32.12	166.2	1101	690.8
VINS	0.1720	0.003012	1120	689.1
VEXT	0.210	0.00312	1130	690.3

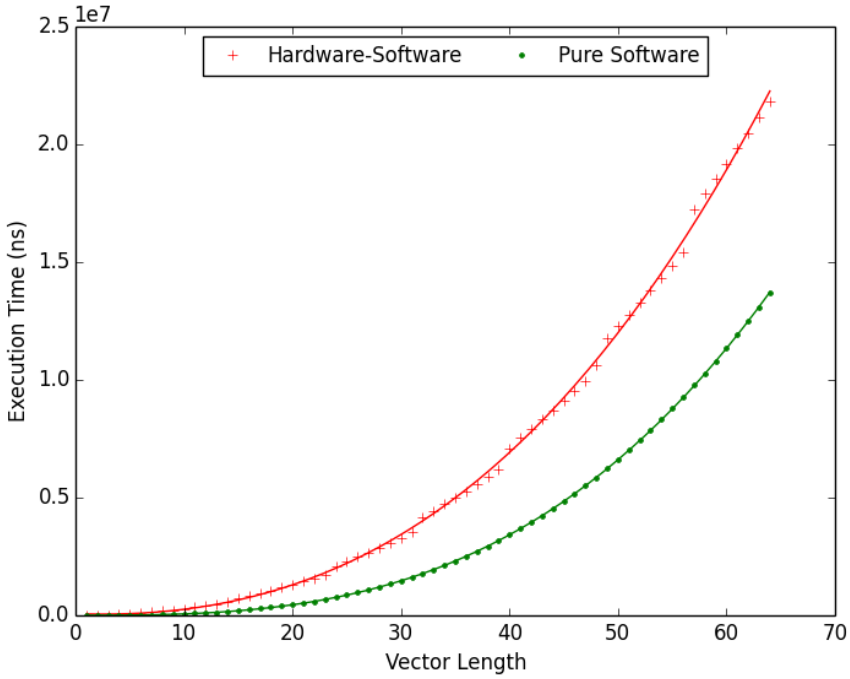

Figure 5.9: Performance of matrix multiplication

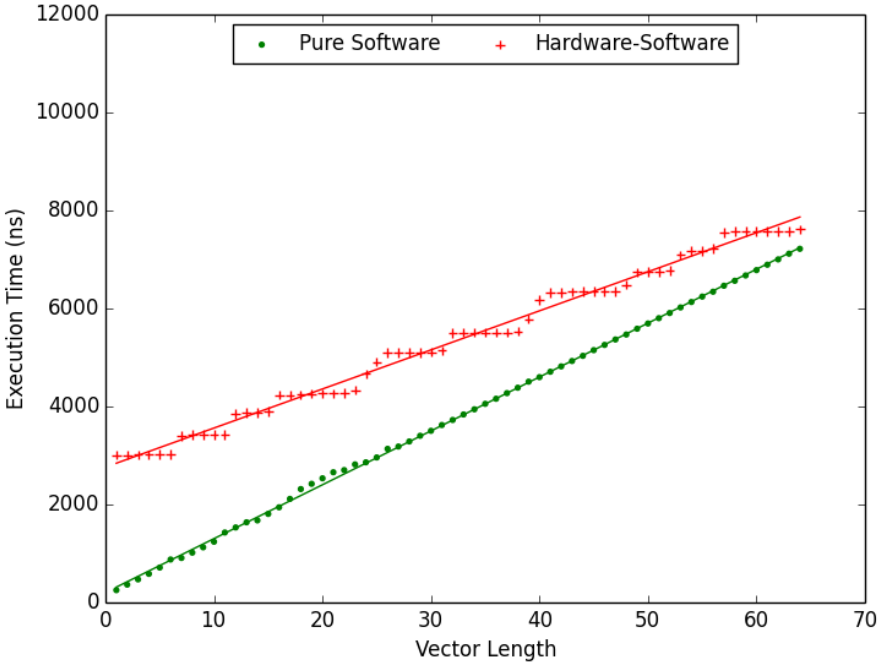

Figure 5.10: Performance of SAXPY

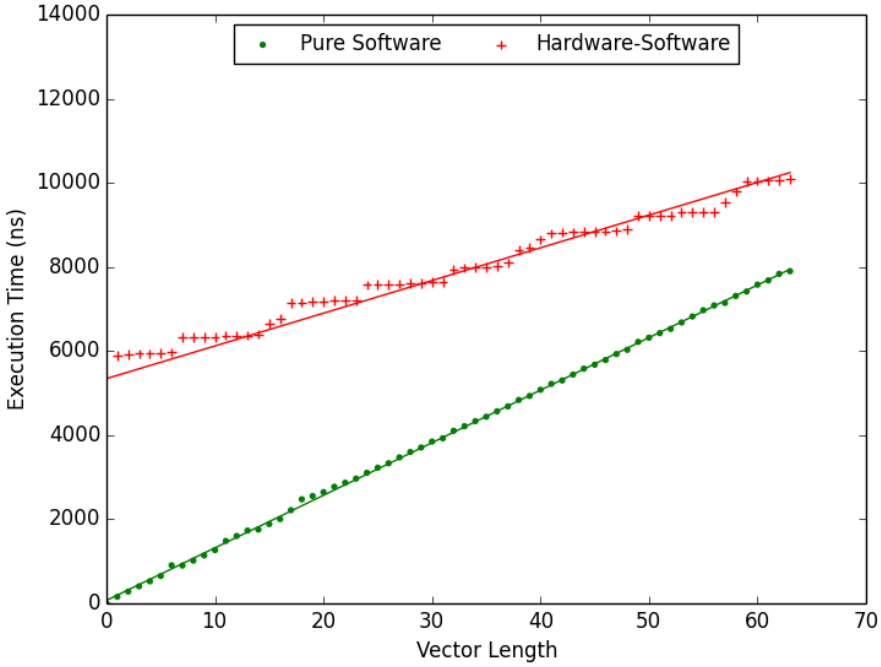

Figure 5.11: Performance of FIR filter

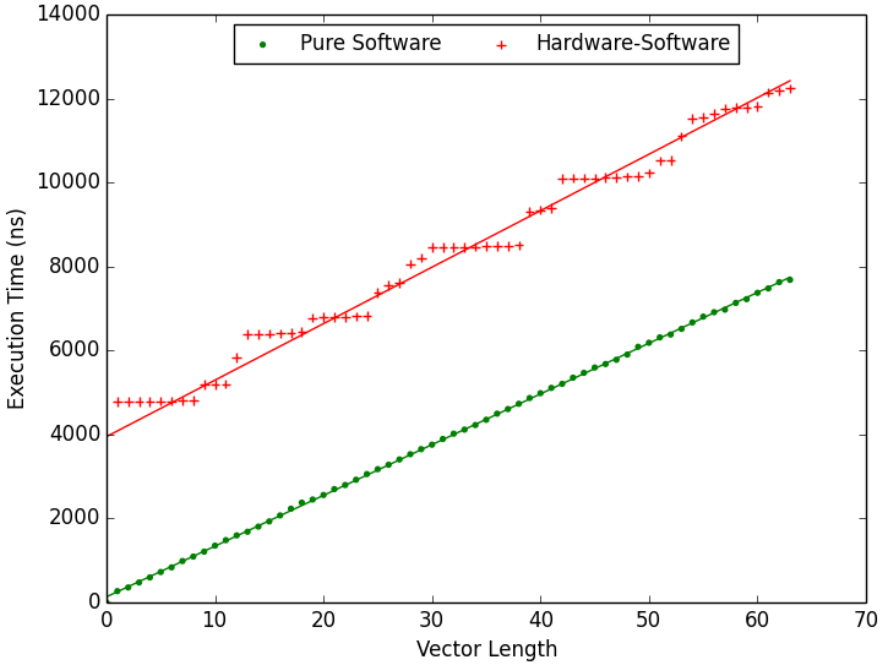

Figure 5.12: Performance of compare and exchange

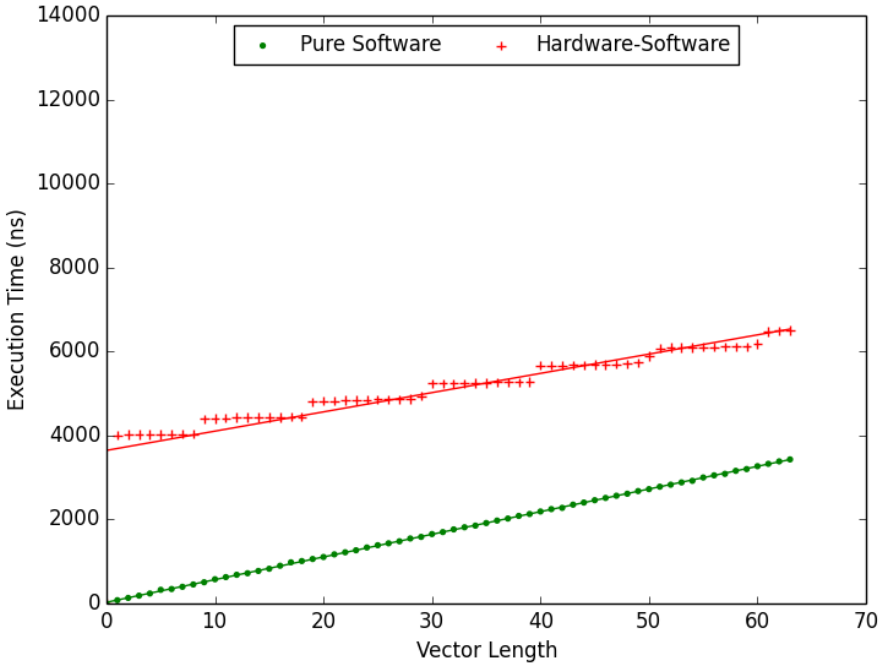

Figure 5.13: Performance of string compare

and compare and exchange is an example of such an application. Further, we also believe that swapping operation can be performed more efficiently on software than on architecture like ours.

The FVP couldn't outperform pure software implementation on any of the benchmarks for vectors of length less than 64. Therefore, we decided to dive further in and examine the result of just performing few operations, like add and multiply involved in these benchmark programs. Figure 5.14, 5.15, and 5.16 show the performance results of add, multiply, and multiply accumulate, respectively on FVP and pure software. Table 5.6 shows the marginal cost (slope) and synchronization cost (y-intercept) of the corresponding graphs. These results are able to capture the effect that we were expecting with our benchmark programs. For all of the three operations, the software implementation starts off as more efficient, but eventually the hardware implementation outperforms the pure software implementation. This effect is empirically captured by the slopes and y-intercepts too. There is a significant overhead of performing any operation on the FVP, indicated by the large y-intercept. However, performing the operation itself is more efficient on the hardware, indicated by small slope. This shows that the communication between the ARM processor and FVP is the biggest bottleneck in our architecture.

Table 5.6: Pure software vs pure hardware performance

Operations	Slope		Y-intercept	
	Pure Hardware	Pure Software	Pure Hardware	Pure Software
Add	30.14	75.23	1084	241.6
Multiply	49.65	76.22	1101	236.2
Multiply Accumulate	49.36	117.1	1108	320.4

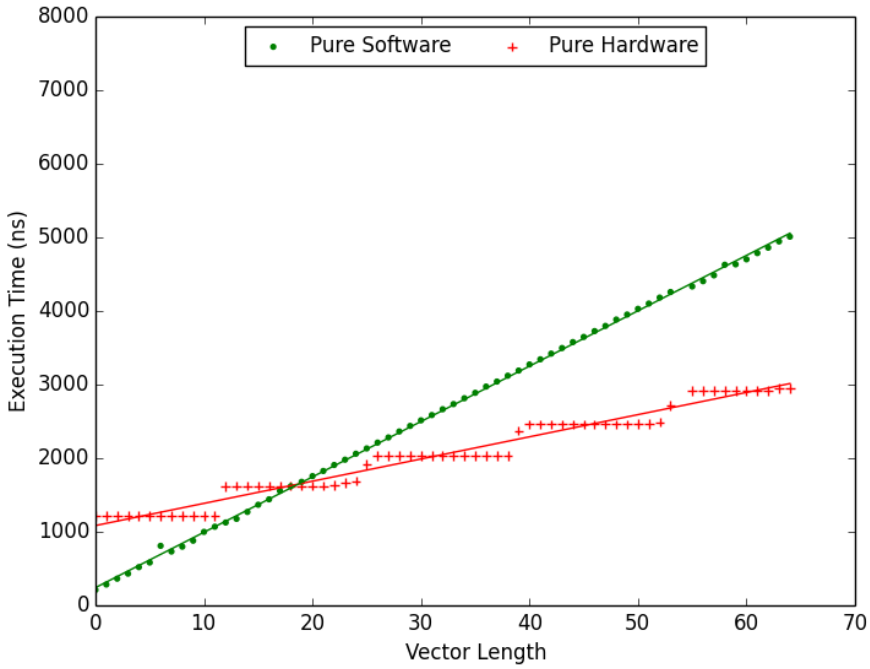

Figure 5.14: Pure Hardware vs Software Implementation of Add

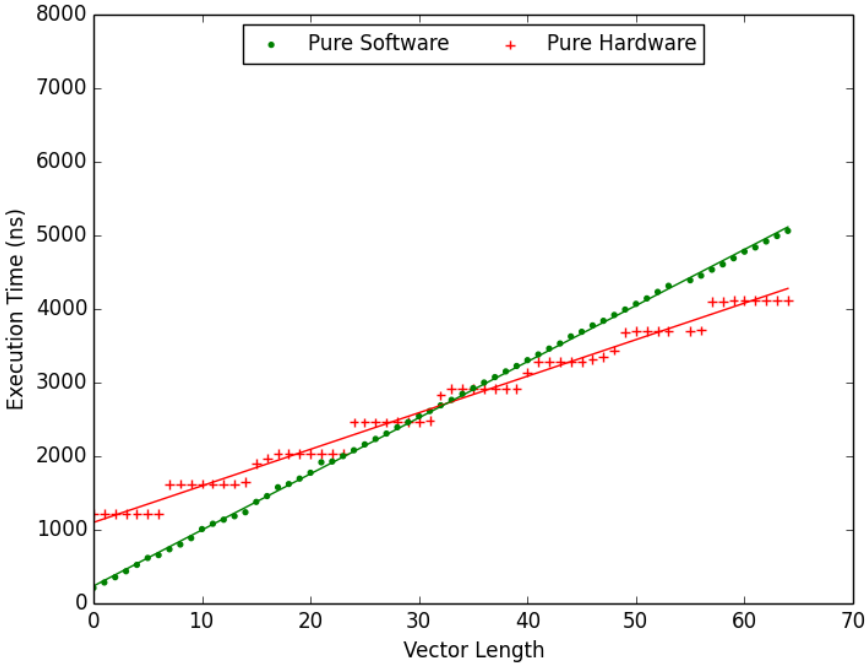

Figure 5.15: Pure Hardware vs Software Implementation of Multiply

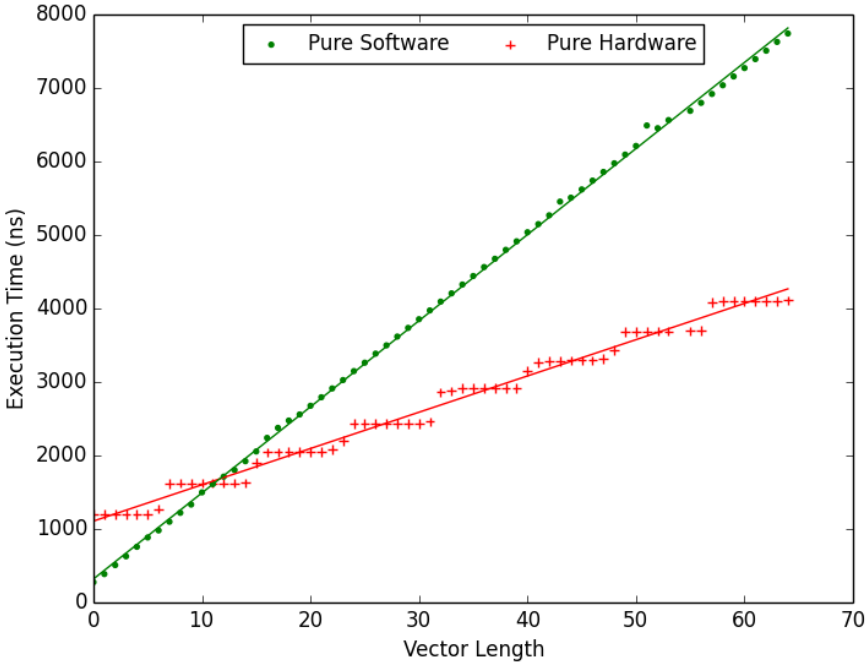

Figure 5.16: Pure Hardware vs Software Implementation of Multiply Accumulate

5.5 Power Analysis

In this section, we examine the power consumed by the hardware implementation of the FVP. There are two types of power consumption in any circuit: static and dynamic, as shown in Figure 5.17. Gate leakage is the main source of static power dissipation on FPGAs [24]. Dynamic power dissipation on FPGAs is caused by signal transitions in the circuit.

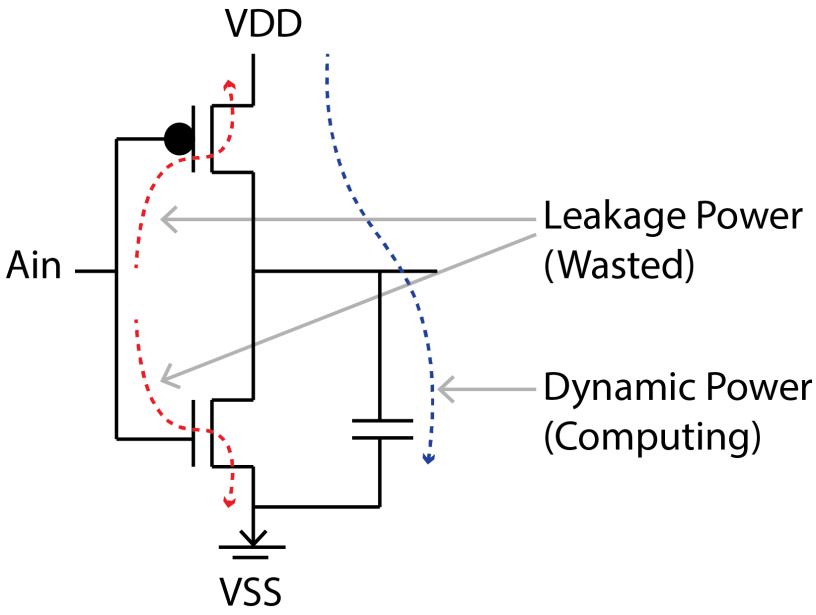

Figure 5.17: Power consumption on a transistor

There are several ways to model and estimate power consumption in digital circuits. Research described in Section 2.5 detail some of the ways to model power consumption in FPGA. For this project, we used Vivado's power analysis tool to estimate the power consumed by the hardware implementation of the FVP. It is a industry standard tool used for power analysis. Figure 5.18 shows the steps in estimating power using the software. Vivado heavily relies on the switching activity of the signals to estimate the power consumption. The information about every element's activity rate can be taken from Value Change Dump (VDC) files which are generated during timing simulations. The current method that Vivado employs is not very accurate for holistic system power estimation. Vivado can only calculate the run-time power consumed by a function after it is mapped on an FPGA. Figure 5.19 shows the estimated power consumed by the design. The average power consumed by out of box ZedBoard is measured at 6.5W [22], and the power consumed by our design is estimated at 1.9W.

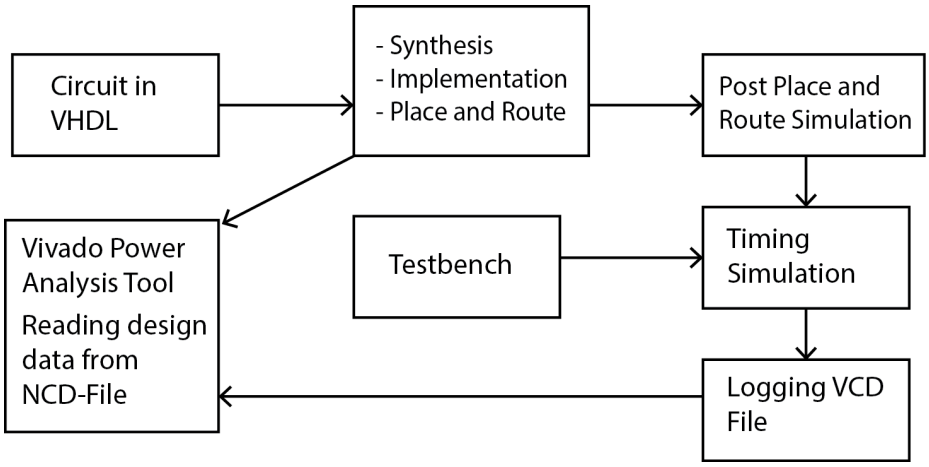

Figure 5.18: Power estimation using Vivado's Power Analysis Tool.

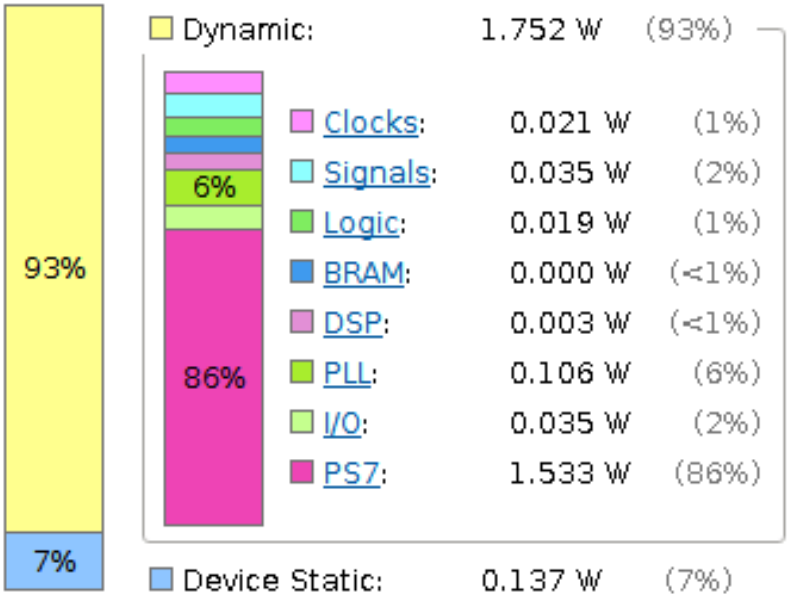

Figure 5.19: Power consumption on the hardware implementation.

We can see from Figure 5.19 that static power accounts for only 7% of the total power consumption. This shows that the design is utilizing most of its power to perform useful computation. Out of the total power spent as dynamic power, majority is consumed by the PS7 IP core. The PS7 IP is the software interface around the ARM processor (PS). It acts as a logic connection between the PS and the PL while assisting user to integrate custom and embedded IPs with the processing system. PS7 IP core is required for every hard-

ware design that interfaces with the ARM. As a result, this overhead power consumption is unavoidable and gives an estimate of the power consumed by the PS in this partnered architecture. Apart from PS7, the components of FVP draw fraction of the total power.

Until recently, performance was the single most important feature of a processor design [9]. Today, however, designers have become more concerned with the power dissipation and in some cases low power consumption is the primary design goal. As a result, just power or performance can not be a good metric to compare processor efficiency. We want to minimize power at a given performance level, or more performance for the same power. Therefore, we need to consider both power and performance to analyze the efficiency of an architecture. The simplest way to do so is by taking the product of energy and delay to get *energy-delay product*. To improve the energy-delay product of an architecture we may either adjust performance or energy consumption. Through our experiments, we were able to deduce that ARM-FVP partnered computation has comparable performance as ARM alone. We believe it also has significantly smaller power footprint than ARM alone, but further experimentation and research is required to solidify this claim. With comparable performance and lower power consumption, our ARM-FVP architecture will have a lower energy-delay product. However, as mentioned earlier, this is just an initial step towards estimate efficiency of a FPGA based co-processor. Some of the possibilities of more detailed analysis is discussed in Chapter 6.

5.6 Summary

The results conclude that the biggest bottleneck in the architecture is the latency in ARM-FVP communication. Despite this overhead involved in communication, the hardware implementation described in Chapter 4 has similar performance efficient as pure software implementation for certain applications. Furthermore, the preliminary power analysis of the design also show that the co-processor draws fraction of the total power supplied to the Zynq. This is a direct evidence that a GPP with tightly coupled reconfigurable co-processors could be more efficient both in terms of energy and performance than pure software as indicated by low energy-delay product. However, there is still lot of room for improvement, further exploration and experimentation. We describe these possibilities in the next section.

6. Future Work

The FVP described in Chapter 4 is a first attempt to show the benefits of using a FPGA-based co-processor system. In this section, we will discuss some of the ways to further improve the FVP and techniques to measure its performance.

6.1 Improving Faux-Vector Processor Design

6.1.1 Upgrading Memory Interface Unit

The memory interface unit used for data transferring in our design is the primary bottleneck in performing any computation on the co-processor. In our current implementation the synchronization time for performing any computation on the co-processor is about 1180 ns, which is significantly higher than performing any computation on a GPP itself. This overhead is the main reason why the pure software implementation of the benchmark programs described in Section 5.4 is faster than than the hybrid implementation. There are few ways to overcome this overhead limitation.

One approach is to implement data pipelining. Pipelining the data transfer would allow computation to begin before all of the data had been read into the FPGA. Pipelining would mitigate the overhead of data transfer by ensuring that after the first set of data had been read, useful computation and not just data transfer would be done during all future transfer cycles. Another approach to reduce the FPGA-host data latency is to make use of Direct Memory Access (DMA) feature supported by many FPGAs. DMA is a FIFO-based method of transferring data between FPGA and a host. The biggest advantage of using DMA is that it doesn't involve the host processor; therefore, it would free the host processor to perform other useful computation during data transfer. As a result, it is faster than other methods of transferring large amount of data. Furthermore, a DMA based approach is optimized to save FPGA resources, and can also automatically synchronize data transfers between the host and a FPGA. The Zynq system used in this project supports different kind of DMA based data transfers, but the usage and properties of these DMA IP cores are

poorly documented.

Another alternative to reduce ARM-FVP communication latency is through instruction pipelining. In the current version of our implementation, the FVP sits idle while the ARM processor is executing instructions. As a consequence, we are not only wasting computational resource but also loosing power efficiency. Therefore, instead of loading one instruction at a time, we could load multiple instructions at a time and only retrieve the results after all the instructions are executed. This would hugely improve the efficiency of our architecture both in terms of power and performance by reducing power consumption and latency from instruction synchronization.

6.1.2 Broadening the Functionality

The current implementation of faux vector processor is very limited in its scope. We currently support operations only on unsigned integers and the operations themselves are limited. Another way to make the FVP more capable would be to increase its scope. Adding support for signed and floating point inputs would allow the vector processor to be used for a much broader set of computation intensive tasks. Unlike other improvements, this would be a trival extension as the co-processor is highly reconfigurable and our system is designed in such a way that users can add more functionality very easily.

6.1.3 Multiple Lane Extension

The current version of FVP only supports single vector lane. As a result, all the computation is performed sequentially. By performing computation sequentially, we are essentially losing potential performance improvement by harnessing the power of parallelism. For the scope of this project, we are focused on energy improvement rather than performance improvement. This leads us to fix the number of lanes of the FVP to single lane. Possible extension to this work could support multiple vector lanes and analyze both the power and performance of such architecture. We believe that adding more vector lanes would definitely improve the performance of the FVP, but it is hard to predict the magnitude of increase in the energy consumption. Future work could possibly look at this performance-energy trade off.

6.1.4 Integration with a Vector Compiler

For a FPGA-based co-processor like FVP to gain widespread use, it must be integrated into compilers. In the current implementation of our system, we are able to provide some

level of abstraction to the user through library calls. However, this still requires the user to first translate their code into vector assembly motivated library calls. If this process is automated by using a vector compiler to target our system, then it would not only provide a higher level or abstraction and ease of use to the users but also increase performance. In the current implementation, the user has to decide what operations are expensive to run on the host processor and on the co-processor. After integrating our architecture with a vector compiler, this process could be automated and compiler can make the decision at runtime whether or not the co-processor should be invoked for a specific instance of a computation. This would maximize efficiency of both programmer and the co-processor.

6.1.5 Automating Circuit Design and Synthesis

As described in Section 3, the process of circuit design, synthesis, and implementation on FPGA is involved. As a result, circuits for frequently used circuits could be automatically generated, installed, and controlled by partial reconfigurable manager. In fact, the processor could evaluate the performance of these circuits, improve their designs, and recompile them into libraries. Over time, such an architecture would specialize each co-processor to its end user without explicit inputs from the user. However, there is still a long way to go before we could build such an architecture as the current state of art software used to program FPGAs are very primitive. Improving these software to program FPGAs is crucial to reaching the ultimate goal of automated circuit design and synthesis.

6.2 Improving Performance Estimation

6.2.1 Improved Power Analysis and Optimization

Power estimation is crucial in hardware devices as it is required to determine weather the device will meet the targeted power specifications. Power analysis of the IP-based system like Zynq is a particularly challenging task at the architecture level because the designers need to compute accurate power estimates without direct knowledge of the IP design details. Dynamic power consumption depends heavily on the design activity when in operation, but many power estimation softwares, like Vivado's power estimation tool, use simulation to estimate the design activity. The problem with this approach is that simulation can mimic the logic of the circuit, but cannot test how the logic will be implemented in the hardware. In this project, we heavily relied on Vivado's power analysis tool to estimate power consumed by our co-processor. However, more detailed power analysis could be performed by using both Vivado's power analysis tool and the techniques from research described in Chapter 2.

Furthermore, there are various power optimizations that could be performed in our faux vector processor design. The current implementation of our design uses the memory interface unit which is not optimized for power as both the FPGA and host has read line to the shared memory constantly high. The architecture could be made more power efficient by switching to an interrupt-based system where FPGA and host communicate via interrupts rather than by comparing instruction IDs.

6.3 Open Challenges

Because of these promising avenues of exploration, we expect the relevance of FPGAs in computing systems to increase in the coming years. Leading market processor manufacturers like Intel are already moving towards integrated configurable logic with commodity CPUs [11]. It is thus no longer a question whether or not FPGAs will appear in mainstream computing systems. Rather, programming community should begin to worry about how the potential of FPGAs can be leveraged to improve performance and energy efficiency.

Several decades of research and development work have matured the software world to a degree that virtually any application field receives a rich set of support by tools, programming languages, libraries, design patterns and good practices. Hardware development, on the other hand, is significantly more complex and has not yet reached the degree of convenience that software developers have long been used to. This is unfortunate not only because potential of hardware technologies like FPGA hasn't been fully realized, but also because hardware-software co-design has, so far, been mostly ignored. Finding a system architecture that brings together the potential of hardware and ease of software development will require a fair amount of experimentation, design, and evaluation. The results from our work are promising, but there is still lot of work to be done to improve the field of hardware-software co-design before it can be attractive for practical use.

7. Conclusions

GPPs are designed for flexibility, with application performance and energy efficiency only as secondary goals. On the other hand, ASIC designs sacrifice flexibility for performance and energy efficiency. Designers of FPGA circuits, however, are not bound to this prioritization. Rather, their circuit typically has to support just one very specific application type and the circuit can be rebuilt whenever it is no longer needed for the current application. Given this freedom, the true potential of FPGA lies in the open space in-between flexibility and efficiency. Most likely, the sweet spot is when different processing units, composed of one or more FPGA units; one or more general-purpose CPUs, operate together in the some form of a hybrid system design. Our design with a dual core ARM processor tightly coupled with a *faux* vector co-processor is a first step towards building such a hybrid system.

The co-processor design described in this work is capable of performing real-world applications. Our preliminary experiments have shown promising results indicating that such a hybrid system would provide flexibility as well as performance and energy efficiency to some extent. Experiments described in Chapter 5 have shown that the bottleneck for a hybrid FPGA-host architecture like ours is the data transfer mechanism. In Chapter 6 we provide some suggestions to improve the data transfer mechanism, and also suggest possible paths for future exploration. Basic energy analysis described in Chapter 5 using Vivado's power analysis tool has estimated that FPGA-based co-processor are efficient at energy utilization and consume only a small fraction of the total power supplied.

Our faux vector processor design and the future work discussed in Chapter 6 provides a first successful attempt in creating a Zynq based FPGA-host hybrid architecture. By further exploring this hardware-software co-design space, we will be able to design architectures with GPP-like flexibility with ASIC-like efficiency.

Acronyms

ALU arithmetic logic units (ALUs) are fundamental processor components that perform arithmetic or bitwise logical functions on binary integer inputs.

ARM advanced RISC machine (ARM) is a set of RISC architectures developed by ARM Holdings. ARM is currently the dominant RISC architecture, and ARM processors are used in most mobile devices.

ASIC application specific integrated circuits (ASICs) are integrated circuits designed for a particular application. They generally cannot be used for other purposes.

AXI Advanced eXtensible Interface (AXI) is a set of micro-controller buses used in the Zynq SoC to handle data transfer between the PS and IP cores on the PL.

BRAM block RAMs that are placed on an FPGA fabric to provide more efficient memory storage for FPGA circuits.

CPU the central processing unit (CPU) performs the instructions of a computer program.

DSP Digital Signal Processor is an IP block in Zynq boards responsible of fast and efficient multiplication and addition.

FPGA field programmable gate arrays (FPGAs) are integrated circuits that can be reconfigured after they have been manufactured.

FVP Faux vector processor is a vector processor that has single lane and executes operations sequentially rather than in parallel.

GPGPU general purpose computing on graphics processing units (GPGPU) refers to using a GPU to execute computation normally performed by the CPU. GPGPU can have better performance than computation on a CPU for applications with large amounts of data parallelism, such as vector processing.

GPP general purpose processors (GPPs) are processors that can be used for a wide variety of programs and applications.

GPU graphics processor units (GPUs) are integrated circuits designed to efficiently process images for output to a display. GPUs exploit data parallelism to achieve much higher performance than CPUs for typical image processing algorithms.

IP intellectual property (IP) cores are how Xilinx defines the individual hardware blocks that can be implemented on their FPGAs.

LUT look-up tables (LUTs) replace computation with indexing into a stored data array. Most computation on FPGAs is implemented through select lines that index into LUTs to encode boolean logic functions.

MIPS microprocessor without interlocked pipeline stages (MIPS) is a RISC instruction set first introduced by MIPS Technologies in 1981.

PL Programmable Logic (PL) is Xilinx's term for FPGA in their architecture.

PS Processing System (PS) is Xilinx's term for ARM processor in their architecture.

RAM random access memory (RAM) is a type of data storage in which read and write times are independent of order of access.

VHDL VHSIC Hardware Description Language (VHDL) is a hardware description language used to define digital systems and integrated circuits. VHDL and Verilog are the two most widely used hardware description languages.

VIRAM VIRAM is a vector extension of MIPS processor and stands for vector intelligent RAM.

Bibliography

[1] Osama T Albaharna, Peter YK Cheung, and Thomas J Clarke. On the viability of fpga-based integrated coprocessors. In *FPGAs for Custom Computing Machines, 1996. Proceedings. IEEE Symposium on*, pages 206–215. IEEE, 1996.

[2] Andrew Canis, Jongsok Choi, Mark Aldham, Victor Zhang, Ahmed Kammoona, Jason H Anderson, Stephen Brown, and Tomasz Czajkowski. Legup: high-level synthesis for fpga-based processor/accelerator systems. In *Proceedings of the 19th ACM/SIGDA international symposium on Field programmable gate arrays*, pages 33–36. ACM, 2011.

[3] Andrew Canis, Jongsok Choi, Mark Aldham, Victor Zhang, Ahmed Kammoona, Tomasz Czajkowski, Stephen D Brown, and Jason H Anderson. Legup: An open-source high-level synthesis tool for fpga-based processor/accelerator systems. *ACM Transactions on Embedded Computing Systems (TECS)*, 13(2):24, 2013.

[4] Eric S. Chung, Peter A. Milder, James C. Hoe, and Ken Mai. Single-chip heterogeneous computing: Does the future include custom logic, FPGAs, and GPGPUs? In *Proceedings of the 2010 43rd Annual IEEE/ACM International Symposium on Microarchitecture*, MICRO '43, pages 225–236, Washington, DC, USA, 2010. IEEE Computer Society. ISBN 978-0-7695-4299-7. doi: 10.1109/MICRO.2010.36. URL `http://dx.doi.org/10.1109/MICRO.2010.36`.

[5] Silviu Ciricescu, Ray Essick, Brian Lucas, Phil May, Kent Moat, Jim Norris, Michael Schuette, and Ali Saidi. The reconfigurable streaming vector processor (rsvptm). In *Proceedings of the 36th annual IEEE/ACM International Symposium on Microarchitecture*, page 141. IEEE Computer Society, 2003.

[6] Vijay Degalahal and Tim Tuan. Methodology for high level estimation of fpga power consumption. In *Proceedings of the 2005 Asia and South Pacific Design Automation Conference*, pages 657–660. ACM, 2005.

[7] Robert H Dennard, VL Rideout, E Bassous, and AR LeBlanc. Design of ion-implanted

mosfet's with very small physical dimensions. *Solid-State Circuits, IEEE Journal of*, 9 (5):256–268, 1974.

[8] Shane T Fleming, Ivan Beretta, David B Thomas, George A Constantinides, and Dan R Ghica. Pushpush: Seamless integration of hardware and software objects via function calls over axi. In *Field Programmable Logic and Applications (FPL), 2015 25th International Conference on*, pages 1–8. IEEE, 2015.

[9] Ricardo Gonzalez and Mark Horowitz. Energy dissipation in general purpose microprocessors. *Solid-State Circuits, IEEE Journal of*, 31(9):1277–1284, 1996.

[10] N. Goulding-Hotta, J. Sampson, G. Venkatesh, S. Garcia, J. Auricchio, P. Huang, M. Arora, S. Nath, V. Bhatt, J. Babb, S. Swanson, and M. Taylor. The GreenDroid mobile application processor: An architecture for silicon's dark future. *Micro, IEEE*, 31(2):86–95, March 2011. ISSN 0272-1732. doi: 10.1109/MM.2011.18.

[11] Prabhat K Gupta. Xeon+ fpga platform for the data center. In *Fourth Workshop on the Intersections of Computer Architecture and Reconfigurable Logic*, volume 119, 2015.

[12] Rehan Hameed, Wajahat Qadeer, Megan Wachs, Omid Azizi, Alex Solomatnikov, Benjamin C. Lee, Stephen Richardson, Christos Kozyrakis, and Mark Horowitz. Understanding sources of inefficiency in general-purpose chips. *SIGARCH Comput. Archit. News*, 38(3):37–47, June 2010. ISSN 0163-5964. doi: 10.1145/1816038.1815968. URL `http://doi.acm.org/10.1145/1816038.1815968`.

[13] Mark D Hill and Michael R Marty. Amdahl's Law in the multicore era. *IEEE Computer*, 41(7):33–38, 2008.

[14] Matthew Jacobsen and Ryan Kastner. Riffa 2.0: A reusable integration framework for fpga accelerators. In *Field Programmable Logic and Applications (FPL), 2013 23rd International Conference on*, pages 1–8. IEEE, 2013.

[15] Ruzica Jevtic and Carlos Carreras. Power measurement methodology for fpga devices. *Instrumentation and Measurement, IEEE Transactions on*, 60(1):237–247, 2011.

[16] Myron King, Jamey Hicks, and John Ankcorn. Software-driven hardware development. In *Proceedings of the 2015 ACM/SIGDA International Symposium on Field-Programmable Gate Arrays*, pages 13–22. ACM, 2015.

[17] Christoforos Kozyrakis and David A Patterson. *Scalable vector media-processors for embedded systems*. University of California, Berkeley, 2002.

[18] Christos Kozyrakis and David Patterson. Overcoming the limitations of conventional vector processors. In *ACM SIGARCH Computer Architecture News*, volume 31, pages 399–409. ACM, 2003.

[19] Ian Kuon and Jonathan Rose. Measuring the gap between FPGAs and ASICs. *Computer-Aided Design of Integrated Circuits and Systems, IEEE Transactions on*, 26(2):203–215, 2007.

[20] Chris Lattner and Vikram Adve. Llvm: A compilation framework for lifelong program analysis & transformation. In *Code Generation and Optimization, 2004. CGO 2004. International Symposium on*, pages 75–86. IEEE, 2004.

[21] David Martin. *Vector Extensions to the MIPS-IV Instruction Set Architecture*. 2000.

[22] Josh Monson, Michael Wirthlin, and Brad L Hutchings. Implementing high-performance, low-power fpga-based optical flow accelerators in c. In *Application-Specific Systems, Architectures and Processors (ASAP), 2013 IEEE 24th International Conference on*, pages 363–369. IEEE, 2013.

[23] Chuck Moore. Data processing in exascale-class computer systems. In *The Salishan Conference on High Speed Computing*, 2011.

[24] Li Shang, Alireza S Kaviani, and Kusuma Bathala. Dynamic power consumption in virtex$^{\text{TM}}$-ii fpga family. In *Proceedings of the 2002 ACM/SIGDA tenth international symposium on Field-programmable gate arrays*, pages 157–164. ACM, 2002.

[25] David B Thomas, Shane T Fleming, George A Constantinides, and Dan R Ghica. Transparent linking of compiled software and synthesized hardware. In *Proceedings of the 2015 Design, Automation & Test in Europe Conference & Exhibition*, pages 1084–1089. EDA Consortium, 2015.

[26] Tim Tuan and Bocheng Lai. Leakage power analysis of a 90nm fpga. In *Custom Integrated Circuits Conference, 2003. Proceedings of the IEEE 2003*, pages 57–60. IEEE, 2003.

[27] Ganesh Venkatesh, Jack Sampson, Nathan Goulding, Saturnino Garcia, Vladyslav Bryksin, Jose Lugo-Martinez, Steven Swanson, and Michael Bedford Taylor. Conservation Cores: Reducing the energy of mature computations. *SIGARCH Comput. Archit. News*, 38(1):205–218, March 2010. ISSN 0163-5964. doi: 10.1145/1735970.1736044. URL `http://doi.acm.org/10.1145/1735970.1736044`.

[28] Ganesh Venkatesh, Jack Sampson, Nathan Goulding-Hotta, Sravanthi Kota Venkata, Michael Bedford Taylor, and Steven Swanson. QsCores: Trading dark silicon for scalable energy efficiency with quasi-specific cores. In *Proceedings of the 44th Annual IEEE/ACM International Symposium on Microarchitecture*, MICRO-44, pages 163–174, New York, NY, USA, 2011. ACM. ISBN 978-1-4503-1053-6. doi: 10.1145/2155620.2155640. URL `http://doi.acm.org/10.1145/2155620.2155640`.

[29] Dong Hyuk Woo and Hsien-Hsin S Lee. Extending amdahl's law for energy-efficient computing in the many-core era. *Computer*, (12):24–31, 2008.

[30] UG585. *Zynq-7000 All Programmable SoC*. Xilinx, v1.8.1 edition, Sept 2014.

[31] Xillybus. URL `http://xillybus.com/`.

[32] Peter Yiannacouras, J Gregory Steffan, and Jonathan Rose. Portable, flexible, and scalable soft vector processors. *Very Large Scale Integration (VLSI) Systems, IEEE Transactions on*, 20(8):1429–1442, 2012.

[33] Jason Yu. *Architecture Specification for Vector Extension to Nios II ISA*. 2008.

[34] Jason Yu, Guy Lemieux, and Christpher Eagleston. Vector processing as a soft-core cpu accelerator. In *Proceedings of the 16th international ACM/SIGDA symposium on Field programmable gate arrays*, pages 222–232. ACM, 2008.

[35] Zedboard. URL `http://zedboard.org/`.